



Sensitivity of PSCs to  
H<sub>2</sub>O and temperature  
changes

F. Khosrawi et al.

# Sensitivity of polar stratospheric cloud formation to changes in water vapour and temperature

F. Khosrawi<sup>1,a</sup>, J. Urban<sup>2,†</sup>, S. Lossow<sup>3</sup>, G. Stiller<sup>3</sup>, K. Weigel<sup>4</sup>, P. Braesicke<sup>3</sup>,  
M. C. Pitts<sup>5</sup>, A. Rozanov<sup>4</sup>, J. P. Burrows<sup>4</sup>, and D. Murtagh<sup>2</sup>

<sup>1</sup>Department of Meteorology, Stockholm University, Stockholm, Sweden

<sup>2</sup>Department of Earth and Space Science, Chalmers University of Technology, Gothenburg, Sweden

<sup>3</sup>Institute of Meteorology and Climate Research, Karlsruhe Institute of Technology, Karlsruhe, Germany

<sup>4</sup>Institute of Environmental Physics, University of Bremen, Bremen, Germany

<sup>5</sup>NASA Langley Research Center, Hampton, USA

<sup>a</sup>now at: Institute of Meteorology and Climate Research, Karlsruhe Institute of Technology, Karlsruhe, Germany

<sup>†</sup>deceased, 14 August 2014

Title Page

Abstract

Introduction

Conclusions

References

Tables

Figures



Back

Close

Full Screen / Esc

Printer-friendly Version

Interactive Discussion



Received: 09 March 2015 – Accepted: 12 June 2015 – Published: 01 July 2015

Correspondence to: F. Khosrawi (farahnaz.khosrawi@kit.edu)

Published by Copernicus Publications on behalf of the European Geosciences Union.

ACPD

15, 17743–17796, 2015

## Sensitivity of PSCs to H<sub>2</sub>O and temperature changes

F. Khosrawi et al.

Title Page

Abstract

Introduction

Conclusions

References

Tables

Figures



Back

Close

Full Screen / Esc

Printer-friendly Version

Interactive Discussion



## Abstract

More than a decade ago it was suggested that a cooling of stratospheric temperatures by 1 K or an increase of 1 ppmv of stratospheric water vapour could promote denitrification, the permanent removal of nitrogen species from the stratosphere by solid polar stratospheric cloud (PSC) particles. In fact, during the two Arctic winters 2009/10 and 2010/11 the strongest denitrification in the recent decade was observed. Sensitivity studies along air parcel trajectories are performed to test how a future stratospheric water vapour ( $\text{H}_2\text{O}$ ) increase of 1 ppmv or a temperature decrease of 1 K would affect PSC formation. We perform our study based on measurements made during the Arctic winter 2010/11. Air parcel trajectories were calculated 6 days backward in time based on PSCs detected by CALIPSO (Cloud Aerosol Lidar and Infrared Pathfinder satellite observations). The sensitivity study was performed on single trajectories as well as on a trajectory ensemble. The sensitivity study shows a clear prolongation of the potential for PSC formation and PSC existence when the temperature in the stratosphere is decreased by 1 K and water vapour is increased by 1 ppmv. Based on 15 years of satellite measurements (2000–2014) from UARS/HALOE, Envisat/MIPAS, Odin/SMR, Aura/MLS, Envisat/SCIAMACHY and SCISAT/ACE-FTS it is further investigated if there is a decrease in temperature and/or increase of water vapour ( $\text{H}_2\text{O}$ ) observed in the polar regions similar to that observed at midlatitudes and in the tropics. Although in the polar regions no significant trend is found in the lower stratosphere, we found from the observations a correlation between cold winters and enhanced water vapour mixing ratios.

## 1 Introduction

Polar stratospheric clouds (PSCs) form in the polar winter stratosphere at altitudes between 15 to 30 km. PSCs consist of liquid and solid particles and have been classified into three different types based on their composition and physical state: (1) Super-

ACPD

15, 17743–17796, 2015

## Sensitivity of PSCs to $\text{H}_2\text{O}$ and temperature changes

F. Khosrawi et al.

Title Page

Abstract

Introduction

Conclusions

References

Tables

Figures



Back

Close

Full Screen / Esc

Printer-friendly Version

Interactive Discussion



## Sensitivity of PSCs to H<sub>2</sub>O and temperature changes

F. Khosrawi et al.

[Title Page](#)[Abstract](#)[Introduction](#)[Conclusions](#)[References](#)[Tables](#)[Figures](#)[Back](#)[Close](#)[Full Screen / Esc](#)[Printer-friendly Version](#)[Interactive Discussion](#)

cooled Ternary Solutions (STS), (2) Nitric Acid Trihydrate (NAT) and (3) ice. The formation of PSCs is strongly temperature dependent. Liquid PSC cloud particles (STS) form by the condensation of water vapour (H<sub>2</sub>O) and nitric acid (HNO<sub>3</sub>) on the liquid stratospheric background sulfate aerosol particles at temperatures 2–3 K below the NAT existence temperature  $T_{\text{NAT}}$  ( $\sim 195$  K) while for the formation of solid cloud particles (ice) much lower temperatures are required, usually 3–4 K below the ice frost point  $T_{\text{ice}}$  ( $\sim 185$  K) (e.g. Carslaw et al., 1994; Koop et al., 1995). The formation of the liquid STS particles is quite well understood, however, the exact formation mechanism of NAT and ice PSC particles still leaves some unresolved questions and is still an active area of research.

Progress in understanding PSC particle formation processes has been made recently in the frame of the European project RECONCILE (Reconciliation of essential process parameters for an enhanced predictability of Arctic stratospheric ozone loss and its climate interactions) (von Hobe et al., 2013). For example, CALIPSO measurements for the Arctic winter 2009/10 presented by Pitts et al. (2011) showed that widespread NAT formation occurred, albeit in low number densities, before ice clouds had been formed at temperatures well above  $T_{\text{ice}}$ . Further, lidar measurements performed during recent years have also indicated that there must be a formation mechanism for NAT PSCs above the ice frost point  $T_{\text{ice}}$  without ice particles necessarily serving as a nucleation kernel for NAT particles. Until the RECONCILE project, the only known pathway to form NAT was through heterogeneous nucleation on ice particles, forming NAT clouds downstream of mountain wave ice clouds (Luo et al., 2003; Fueglistaler et al., 2003; Höpfner et al., 2006).

Heterogeneous nucleation on particles such as meteoric smoke has been suggested to be a potential pathway for NAT formation (Bogdan et al., 2003; Voigt et al., 2005). Hoyle et al. (2013) performed box model simulations along air parcel trajectories based on the observations by CALIPSO made during the Arctic winter 2009/10 applying a new parameterisation for heterogeneous NAT nucleation, assuming NAT formation on particles as e.g. meteoric smoke. The CALIPSO observations were well reproduced by

## Sensitivity of PSCs to H<sub>2</sub>O and temperature changes

F. Khosrawi et al.

Title Page

Abstract

Introduction

Conclusions

References

Tables

Figures



Back

Close

Full Screen / Esc

Printer-friendly Version

Interactive Discussion



the model simulations applying this new parameterization thus indicating that NAT nucleation on other particles than ice is possible. Further, both the modelling study by Hoyle et al. (2013) and the one by Engel et al. (2013) using the Zurich Optical and Microphysical box Model (ZOMM) showed that small-scale temperature fluctuations usually not represented in meteorological data needed to be considered to reproduce the CALIPSO observations.

Denitrification, the permanent removal of HNO<sub>3</sub> by sedimenting polar stratospheric cloud particles, limits the deactivation process of the ozone destroying substances in springtime and thus leads to a prolongation of the ozone destroying cycles. Stratospheric cooling caused by increasing greenhouse gas concentrations will have significant implications on denitrification and ozone loss. Model simulations predict that very large ozone losses will occur more frequently in the future in the Arctic and that the recovery of the ozone layer will be delayed by more than a decade due to increased greenhouse gas concentrations (e.g. Austin et al., 1992; Shindell et al., 1998; Eyring et al., 2010; SPARC CCMVal, 2010).

Water vapour is one of the most important greenhouse gases and plays a key role in the chemistry and radiative balance of the upper troposphere and lower stratosphere (UT/LS). Long-term balloon-borne measurements indicate an increase of the stratospheric water vapour abundance by an average of 1 ppmv during the last 30 years (1980–2010) in the tropics and at mid-latitudes (Scherer et al., 2008; Hurst et al., 2011). Merged satellite data sets covering the period from 1988–2010, however, do not confirm the trend found in the Boulder time series and it has been suggested that the trends over Boulder cannot be considered as representative of the global stratosphere. Although a significantly negative trend was found in the lower stratosphere, a significantly positive trend was found in the upper stratosphere (Hegglin et al., 2014).

Dessler et al. (2014) analysed satellite data together with a trajectory model. They did not see any firm evidence of trends (neither positive nor negative) in the data since the mid 1980s. However, they cannot rule out that a trend exists that is just too small to be identified given the large inter-annual and interdecadal variability. Gettelman



low  $T_{\text{NAT}}$  or  $T_{\text{ice}}$  along the trajectories are considered for a water vapour increase of up to 1 ppmv and a temperature decrease of up to 1 K in the stratosphere. (2) Measurements from several different satellites together with temperatures from ECMWF are used to investigate water vapour trends and variability in the polar stratosphere. So far trend studies in stratospheric water vapour have focused on the tropics and mid-latitudes. Here, for the first time such an analyses has been performed for the polar stratosphere. We use satellite measurements that were derived for the 15 year period 2000–2014.

## 2 Satellite data

To investigate a possible water vapour trend as well as water vapour variability in the polar lower stratosphere, satellite observations of water vapour from the Odin Sub-Millimetre Radiometer (Odin/SMR), the Aura Microwave Limb Sounder (Aura/MLS), the Envisat Michelson Interferometer for Passive Soundings (Envisat/MIPAS), the SCanning Imaging Absorption spectroMeter for Atmospheric CHartographyY (Envisat/SCIAMACHY), the SCISAT Atmospheric Chemistry Experiment Fourier Transform Spectrometer (SCISAT/ACE-FTS) and the UARS Halogen Occultation Experiment (UARS/HALOE) are used. A short description of these satellite instruments will follow below. A detailed intercomparison of water vapour derived from these instruments can be found in Hegglin et al. (2013). For performing case studies along air parcel trajectories that are based on PSC measurements we apply measurements from the Cloud-Aerosol Lidar with Orthogonal Polarization (CALIOP) on board of CALIPSO (Cloud-Aerosol Lidar and Infrared Pathfinder Satellite Observations).

### 2.1 Odin/SMR

Odin/SMR was launched on 20 February 2001 and observes the thermal emission of trace gases from the Earth's limb. Odin carries two instruments, the Optical Spec-

## Sensitivity of PSCs to H<sub>2</sub>O and temperature changes

F. Khosrawi et al.

Title Page

Abstract

Introduction

Conclusions

References

Tables

Figures

◀

▶

◀

▶

Back

Close

Full Screen / Esc

Printer-friendly Version

Interactive Discussion



## Sensitivity of PSCs to H<sub>2</sub>O and temperature changes

F. Khosrawi et al.

Title Page

Abstract

Introduction

Conclusions

References

Tables

Figures



Back

Close

Full Screen / Esc

Printer-friendly Version

Interactive Discussion



trograph and Infrared Imaging System (OSIRIS) (Llewellyn et al., 2004) and the Sub-Millimetre Radiometer (SMR) (Frisk et al., 2003). Observations by Odin/SMR were performed in a time-sharing mode with astronomical observations until 2007 and solely in aeronomy mode thereafter. In aeronomy mode, various target bands are dedicated to profile measurements of trace constituents relevant to stratospheric and mesospheric chemistry and dynamics such as O<sub>3</sub>, ClO, N<sub>2</sub>O, HNO<sub>3</sub>, H<sub>2</sub>O, CO, HO<sub>2</sub> and NO, as well as minor isotopologues of H<sub>2</sub>O and O<sub>3</sub> (e.g. Murtagh et al., 2002). Stratospheric mode measurements were performed every third day until April 2007 and every other day thereafter. A typical stratospheric mode scan covers the altitude range from 7 to 70 km with a resolution of ~ 1.5 km in terms of tangent altitude below 50 km and of ~ 5.5 km above. Usually, the latitude range between 82.5° S and 82.5° N is observed (Urban et al., 2005b, a). Water vapour measurements are derived by Odin/SMR in several different bands in the sub-millimetre range. Here, level-2 data from the 544.6 GHz band of version 2.0 for the lower stratosphere are used (Urban et al., 2007, 2012; Urban, 2008).

## 2.2 Aura/MLS

MLS on board Aura is part of the NASA/ESA “A-train” satellite constellation. MLS was launched in July 2004 and is an advanced successor of the MLS instrument on the Upper Atmosphere Research Satellite (UARS) that was launched in 1991 and provided measurements until 1999. MLS is a limb sounding instrument that measures the thermal emission at millimetre and sub-millimetre wavelengths using seven radiometers to cover five broad spectral regions (Waters et al., 2006). Measurements are performed from the surface to 90 km with a global latitude coverage from 82° S to 82° N. Global water vapour measurements are derived from a line close to the 183 GHz band (Lambert et al., 2007). Version 3.3 data is used in this study (Hurst et al., 2014).

## 2.3 Envisat/MIPAS

MIPAS is a middle infrared Fourier transform spectrometer and was launched in March 2002 on board Envisat. MIPAS was operational until the sudden loss of contact with Envisat on 8 April 2012. MIPAS measured the atmospheric emission spectrum in the limb sounding geometry. MIPAS operated in its nominal observation mode from June 2002 to March 2004, thus approximately two years. Measurements during this time period were performed in its full spectral resolution measurement mode with a designated spectral resolution of  $0.035 \text{ cm}^{-1}$ . Measurements were performed covering the altitude range from the mesosphere to the troposphere with a high vertical resolution (about 3 km in the stratosphere). After a failure of the interferometer slide at the end of March 2004, MIPAS resumed measurements in January 2005 with a reduced spectral resolution of  $0.0625 \text{ cm}^{-1}$ , but with improved spatial resolution. Data products of MIPAS are up to 30 trace species, e.g.  $\text{H}_2\text{O}$ ,  $\text{O}_3$ ,  $\text{HNO}_3$ ,  $\text{CH}_4$ ,  $\text{N}_2\text{O}$ ,  $\text{NO}_2$  as well as temperature (Fischer and Oelhaf, 1996; Fischer et al., 2008). Here, the MIPAS data version V5H\_H2O\_20 and V5R\_H2O\_220/221 derived with the IMK/IAA retrieval processor covering the periods 2002–2003 and 2005–April 2011/May 2011–2012, respectively, have been used (updated version of the retrieval as described in Milz et al., 2009; von Clarmann et al., 2009).

## 2.4 Envisat/SCIAMACHY

SCIAMACHY was launched on board Envisat in March 2002 and was in operation from August 2002 until the sudden loss of contact with Envisat on 8 April 2012. SCIAMACHY observed electromagnetic radiation upwelling from the Earth's atmosphere in 3 measurement modes: occultation, nadir, and limb geometry. The instrument and mission objectives are provided by Burrows et al. (1995) and Bovensmann et al. (1999). In this study, measurements of the scattered solar light in limb viewing geometry are used. In this geometry, the instrument scanned the horizon in 3.3 km steps from  $-3$  to 92 km (0 to 92 km since October 2010). This vertical sampling and the instantaneous field of

### Sensitivity of PSCs to $\text{H}_2\text{O}$ and temperature changes

F. Khosrawi et al.

Title Page

Abstract

Introduction

Conclusions

References

Tables

Figures



Back

Close

Full Screen / Esc

Printer-friendly Version

Interactive Discussion





## 2.6 UARS/HALOE

The HALogen Occultation Experiment (HALOE) was launched aboard the Upper Atmosphere Research Satellite (UARS). HALOE is as ACE-FTS a solar occultation instrument (Russell et al., 1993). The geometry of the UARS orbit (57° inclination, circular at 585 km with orbit period of 96 min) results in 15 sunrise and 15 sunset measurements daily. Measurements between 80° N and 80° S in about 45 days are performed. HALOE was launched in September 1991 and provided measurements until 2005, thus over a time period of 14 years (Harris et al., 1996). Therefore, HALOE provides the longest satellite data set though it is not used to its full extent in this study since we focus on measurements obtained since the millennium. HALOE Version 19 data is used in this study.

## 2.7 CALIPSO/CALIOP

CALIPSO is part of the NASA/ESA “A-train” satellite constellation and has been in operation since June 2006. Measurements of PSCs are provided by CALIOP (Pitts et al., 2009). CALIOP is a two-wavelength, polarisation sensitive lidar. High vertical resolution profiles of the backscatter coefficient at 532 and 1064 nm as well as two orthogonal (parallel and perpendicular) polarisation components at 532 nm are provided (Winker et al., 2007; Pitts et al., 2007). The lidar pulse rate is 20.25 Hz, corresponding to one profile every 333 m horizontally. The vertical resolution of CALIOP varies with altitude from 30 m in the lower troposphere to 180 m in the stratosphere. For the PSC analyses, the CALIPSO profile data are averaged to a resolution of 180 m vertically and 5 km horizontally. The determination of the composition of PSCs is based on the measured aerosol depolarisation ratio (ratio of parallel and perpendicular components of 532 nm backscatter) and the inverse scattering ratio ( $1/R_{532}$ ), where  $R_{532}$  is the ratio of the total to molecular backscatter at 532 nm (Pitts et al., 2007, 2009). Using these two quantities, PSCs are classified into: STS, water ice, and three classes of liquid/NAT mixtures (Mix-1, Mix-2 and Mix-2 enhanced). Mix-1 denotes mixtures with very low NAT number

Title Page

Abstract

Introduction

Conclusions

References

Tables

Figures



Back

Close

Full Screen / Esc

Printer-friendly Version

Interactive Discussion



## Sensitivity of PSCs to H<sub>2</sub>O and temperature changes

F. Khosrawi et al.

[Title Page](#)[Abstract](#)[Introduction](#)[Conclusions](#)[References](#)[Tables](#)[Figures](#)[Back](#)[Close](#)[Full Screen / Esc](#)[Printer-friendly Version](#)[Interactive Discussion](#)

densities (from about  $3 \times 10^{-4}$  to  $10^{-3} \text{ cm}^{-3}$ ), Mix-2 denotes mixtures with intermediate NAT number densities of ( $10^{-3} \text{ cm}^{-3}$ ), and Mix-2 enhanced denotes mixtures with sufficiently high NAT number densities ( $> 0.1 \text{ cm}^{-3}$ ) and volumes ( $> 0.5 \mu\text{m}^3 \text{ cm}^{-3}$ ) that their presence is not masked by the more numerous STS droplets at temperatures well below  $T_{\text{NAT}}$ . In addition, intense mountain-wave induced ice PSCs are identified as a subset of CALIPSO ice PSCs through their distinct optical signature in  $R_{532}$  (Pitts et al., 2011).

### 3 Arctic winter 2010/11

The Arctic winter 2010/11 was one of the coldest in the last two decades (Manney et al., 2011; Sinnhuber et al., 2011). The 2010/11 winter was characterised by an anomalously strong vortex with an atypically long cold period that was persistent from mid-December to mid-March (Manney et al., 2011). The polar vortex formed at the end of November 2010 and remained stable until the end of April. The long cold period, lasting over four months, was interrupted by short warmer periods in the beginning of January, February and March due to minor warmings. In February and March, temperatures were colder than in previous years of the last decade. The final warming during the 2010/11 Arctic winter occurred in mid-April, thus later than usual (Arnone et al., 2012; Kuttipurath et al., 2012).

The PSC season during the 2010/11 winter can be divided into four PSC phases according the four cold phases that occurred over the four month period from December 2010 to March 2011. The time periods of these four phases and the PSC types that occurred during each phase were derived from CALIPSO observations and are as follows (Khosrawi et al., 2012): (1) 23 December 2010 to 8 January 2011: STS, Mix 1/2 and ice clouds. (2) 20–28 January 2011: mainly Mix-1 and Mix-2 with some STS and ice. (3) 5–27 February: STS, Mix-1 and Mix-2 as well as ice clouds. (4) 5–19 March: STS clouds (Note: no CALIPSO data is available from 8 to 13 March).

## Sensitivity of PSCs to H<sub>2</sub>O and temperature changes

F. Khosrawi et al.

Title Page

Abstract

Introduction

Conclusions

References

Tables

Figures



Back

Close

Full Screen / Esc

Printer-friendly Version

Interactive Discussion



A graphic presentation of the temporal evolution of time,  $V_{\text{PSC}}$ ,  $T - T_{\text{NAT}}$  and several trace gases during this winter can be found in Arnone et al. (2012) and Kuttipurath et al. (2012). Arnone et al. (2012) performed a similar analysis on PSC occurrence as we did, but used MIPAS observations for PSC detection. They also derive four PSC phases from MIPAS, however with somewhat different time periods for each phase as the ones we derive from CALIPSO. Differences in PSC detection between both instruments are caused by the different measurement principle (active lidar in the visible vs. passive spectroscopy in the infrared spectral region). CALIPSO generally detects PSCs in a greater fraction than MIPAS. This can be explained by the patchier nature of PSCs in the Arctic and the different spatial resolutions of the two instruments, which makes the clouds more likely to be detected by the CALIPSO lidar (Höpfner et al., 2009). The Arctic winter 2010/11 has been well analysed, especially with respect to ozone loss (Manney et al., 2011; Sinnhuber et al., 2011; Arnone et al., 2012; Kuttipurath et al., 2012; Hommel et al., 2014) while the dynamical perspective, thus the exceptional dynamical conditions of this winter so far were only discussed in detail by Hurwitz et al. (2011).

## 4 Sensitivity studies

The sensitivity study is performed based on measurements of PSCs by CALIPSO during the Arctic winter 2010/11. The basic approach is demonstrated on single trajectories, but the final results rely on a statistical assessment of a trajectory ensemble. Based on the PSCs observed by CALIPSO during the Arctic winter 2010/11 air parcel trajectories were calculated 6 days backwards with the NOAA HYSPLIT (Hybrid Single Particle Lagrangian Integrated Trajectory Model) model based on GDAS (Global Data Assimilation System) analyses<sup>1</sup>. GDAS analyses are provided by the National Center for Environmental Predictions (NCEP) four times a day (00:00, 06:00, 12:00

<sup>1</sup><http://ready.arl.noaa.gov/HYSPLIT.php>

and 18:00 UTC) with a horizontal resolution of  $1^\circ \times 1^\circ$  on 23 pressure levels (1000 to 20 hPa). An isentropic method was used for the calculation of vertical motion. The trajectories were started for each PSC detection at three different altitudes, corresponding to the bottom, middle and top of the cloud.

The Arctic winter 2010/11 has been chosen for the sensitivity study because it was one of the coldest Arctic winters leading to a high number of PSC occurrences. This makes the statistics more reliable than if we would have chosen a warmer winter with less PSC occurrences. During the Arctic winter 2010/11 PSCs were detected by CALIPSO on 47 days on 259 orbit tracks. In total, 738 trajectories were calculated according to the CALIPSO observations and considered for the sensitivity study on the trajectory ensemble. For the sensitivity study on single trajectories we selected two trajectories, one trajectory where temperatures below  $T_{\text{NAT}}$  were reached, but not below  $T_{\text{ice}}$  and one where temperatures below both,  $T_{\text{NAT}}$  and  $T_{\text{ice}}$ , were reached along the trajectory. Figure 1 shows a map with locations where the trajectories were started according to the PSCs detected by CALIPSO, colour coded by the four cold phases during the Arctic winter 2010/11. PSCs were observed around Greenland during Phase 1, during Phase 2 PSCs were observed over Russia and during Phase 3 over the entire Arctic. During Phase 4 only a few PSCs were detected which were located around Greenland<sup>2</sup>.

## 4.1 Sensitivity studies on single back trajectories

### 4.1.1 Case 1: sensitivity to H<sub>2</sub>O enhancements

Figure 2 shows the CALIPSO measurement on 26 February 2011 around 00:04 UTC. A PSC was measured at altitudes between 16 and 24 km (between 76° N 61° E to 70° N 49° E). The PSC was located east of Novaya Zemlya and was composed of all kinds of PSC particles but mainly of STS with a thick ice layer in between (Fig. 2). Based on

<sup>2</sup>Note: no CALIPSO observations are available from 8 to 13 March.

## Sensitivity of PSCs to H<sub>2</sub>O and temperature changes

F. Khosrawi et al.

Title Page

Abstract

Introduction

Conclusions

References

Tables

Figures



Back

Close

Full Screen / Esc

Printer-friendly Version

Interactive Discussion



the PSC observed on 26 February 2011 air parcel trajectories were calculated 6 days backwards with the HYSPLIT model. The trajectories were started at 00:00 UTC at 20, 22 and 24 km (started at 71° N 61° E) and ended at 20 February at 00:00 UTC.

Figure 3 shows the temperature along the trajectory started at 20 km (black line) together with the threshold temperatures for  $T_{\text{NAT}}$  and  $T_{\text{ice}}$  (red solid and dashed line, respectively). The threshold temperatures were calculated according to the parameterisations of Marti and Mauersberger (1993) and Hanson and Mauersberger (1988), respectively.  $T_{\text{NAT}}$  and  $T_{\text{ice}}$  were calculated for 5 ppmv (typical water mixing ratio during polar winter) and for increased water vapour mixing ratios of 5.5 and 6 ppmv, respectively. Along the trajectory temperatures drop twice below  $T_{\text{NAT}}$  (at  $t = -140$  to  $-100$  h, temperature range  $T_1$ , and at  $t = -20$  to  $0$  h, temperature range  $T_2$ ) but temperatures did not reach  $T_{\text{ice}}$ . The temperature history along the trajectory is in agreement with the CALIPSO observations. Although ice was measured on that day, the ice layer was located in the middle of the PSC, between 21 and 23 km. The trajectory considered here was started at 20 km, thus at the bottom of the PSC and therefore below the ice layer (Fig. 2). With increasing  $\text{H}_2\text{O}$  mixing ratio the  $T_{\text{NAT}}$  threshold temperature is higher and temperatures can more easily drop below  $T_{\text{NAT}}$ . However, a slight prolongation of temperatures below  $T_{\text{NAT}}$  is found only for the temperature range  $T_1$  (Table 1). Although the effect on  $T_{\text{NAT}}$  seems to be insignificant in this example, the effect on  $T_{\text{ice}}$  seems to be more significant. Temperatures did not drop below  $T_{\text{ice}}$  but came very close to the  $T_{\text{ice}}$  threshold when water vapour mixing ratios were increased. Therefore, another trajectory has been chosen, one where  $T_{\text{ice}}$  was reached along the trajectory using a water vapour mixing ratio of 5 ppmv (typical water vapour mixing ratio during polar winter). This trajectory is discussed in the following section.

#### 4.1.2 Case 2: sensitivity to $\text{H}_2\text{O}$ enhancements and additional cooling

Figure 4 shows the CALIPSO measurement on 23 January 2011. A PSC was measured over Russia at altitudes between 16 and 23 km (80° N 139° E to 66° N 105° E). Based on the PSC measured on 23 January 2011, back trajectories were calculated

## Sensitivity of PSCs to $\text{H}_2\text{O}$ and temperature changes

F. Khosrawi et al.

Title Page

Abstract

Introduction

Conclusions

References

Tables

Figures



Back

Close

Full Screen / Esc

Printer-friendly Version

Interactive Discussion



with HYSPLIT 6 days backwards starting at 20:00 UTC at three different altitudes within the PSC, namely at 18, 20 and 22 km (started at 72° N 113° E). As in the previous example, the PSC was composed of all kinds of PSC particles, but STS, Mix 2 enhanced (liquid/NAT mixture with intermediate NAT number densities of  $10^{-3} \text{ cm}^{-3}$ ) and some ice in between was dominating (Fig. 4).

Figure 5 shows the temperature along the trajectory (black) that was started at 18 km as well as the threshold temperatures for  $T_{\text{NAT}}$  and  $T_{\text{ice}}$  (red solid and dashed line, respectively). As in the case discussed in Sect. 4.1.1, the threshold temperatures were calculated for 5 ppmv (typical water mixing ratio during polar winter (Achtert et al., 2011 and references therein, Khosrawi et al., 2011) and for increased water vapour mixing ratios of 5.5 and 6 ppmv (middle and bottom panel). The temperatures drop in this case twice below  $T_{\text{NAT}}$  along the trajectory, at  $t = -135$  to  $-105$  h (temperature range  $T_1$ ) and  $t = -45$  to 0 h (temperature range  $T_2$ ). Temperatures during the second time period with  $T_2 < T_{\text{NAT}}$  where colder and even reached  $T_{\text{ice}}$ . The time periods where temperatures were lower than  $T_{\text{NAT}}$  are prolonged when the atmospheric water vapour mixing ratio is increased (Table 2). For example, while the  $T_1$  temperatures did not reach below  $T_{\text{NAT}}$  under normal stratospheric conditions, temperatures reach 15 and 30 h below  $T_{\text{NAT}}$  for a increase in  $\text{H}_2\text{O}$  mixing ratio of 0.5 and 1 ppmv, respectively, thus allowing STS and NAT PSC formation and existence during a longer time period.

The effect becomes even stronger when additionally the temperature is decreased (Fig. 6). Time periods where  $T_1$  or  $T_2$  are below  $T_{\text{NAT}}$  and  $T_{\text{ice}}$  become much longer, as can be seen from Table 2. Further, the effect becomes more pronounced for  $T_{\text{ice}}$  as can be expected, but there seems to be also an increase in  $T_2$  below  $T_{\text{NAT}}$  due to strong temperature cooling along the trajectory.

## 4.2 Sensitivity studies on back trajectory ensemble

The back trajectory ensemble was calculated starting at dates and times when PSCs were measured by CALIPSO during the Arctic winter 2010/11. For each PSC measurement, trajectories were calculated 6 days backward in time at three different altitudes,

## Sensitivity of PSCs to $\text{H}_2\text{O}$ and temperature changes

F. Khosrawi et al.

Title Page

Abstract

Introduction

Conclusions

References

Tables

Figures



Back

Close

Full Screen / Esc

Printer-friendly Version

Interactive Discussion



corresponding to the top, middle and bottom of the cloud. In total 738 trajectories were calculated. During the course of the 6 days the trajectories in general followed the circular flow within the polar vortex and thus the air masses were transported once around in the polar regions. The temperatures along the trajectories derived with HYSPLIT are in good agreement with the corresponding PSC types measured by CALIPSO.

Using the entire trajectory ensemble the total time (sum over all 738 trajectories) where the temperature was below  $T_{\text{NAT}}$  and  $T_{\text{ice}}$ , respectively, was estimated assuming an  $\text{H}_2\text{O}$  mixing ratio of 5 ppmv. This calculation was repeated assuming a  $\text{H}_2\text{O}$  increase of 0.25–1 ppmv ( $\Delta\text{H}_2\text{O} = 0.25$  ppmv) as well as a decrease in temperature by 0.5 and 1 K. Additionally, the calculation was repeated for a water vapour decrease of 0.25 ppmv to also investigate what the effect of an opposite change would be, which could result from the natural  $\text{H}_2\text{O}$  variability. To quantify the effect a change in  $\text{H}_2\text{O}$  mixing ratio and a decrease in temperature would have, we calculated the enhancement in time that would result where the temperatures would be exposed to temperatures below  $T_{\text{NAT}}$  and  $T_{\text{ice}}$ .

The results of the sensitivity study with the trajectory ensemble are summarised in Figs. 7 and 8 for  $T_{\text{NAT}}$  and in Figs. 9 and 10 for  $T_{\text{ice}}$ . In Figs. 7 and 9 the total time the temperature is below  $T_{\text{NAT}}$  and  $T_{\text{ice}}$ , respectively, is given while in Figs. 8 and 10 the additional time is given the temperature would be below  $T_{\text{NAT}}$  and  $T_{\text{ice}}$ , respectively, if the  $\text{H}_2\text{O}$  mixing ratio would increase and temperature decrease (see also tables in Supplement). The calculation of extra exposure time to  $T_{\text{NAT}}$  and  $T_{\text{ice}}$  was done assuming  $\text{HNO}_3$  mixing ratios of 7, 5 and 3 ppmv which corresponds to the conditions in the polar lower stratosphere at the beginning of the winter and later in the winter when  $\text{HNO}_3$  has been taken up by the PSCs and  $\text{HNO}_3$  has been permanently removed by sedimenting PSC particles (denitrification).

For the reference conditions (normal stratospheric winter conditions, beginning of the winter, thus prevailing gas phase abundances of 5 ppmv  $\text{H}_2\text{O}$  and 7 ppmv  $\text{HNO}_3$ ) temperatures were in total below  $T_{\text{NAT}}$  for 43 512 h (Fig. 7). Note: total trajectory time is 107 010 h (738 trajectories  $\times$  145 h). If  $\text{HNO}_3$  decreases during the course of the

## Sensitivity of PSCs to $\text{H}_2\text{O}$ and temperature changes

F. Khosrawi et al.

Title Page

Abstract

Introduction

Conclusions

References

Tables

Figures



Back

Close

Full Screen / Esc

Printer-friendly Version

Interactive Discussion



winter to 5 ppbv the air will be  $\sim 3600$  h less exposed to temperatures below  $T_{\text{NAT}}$ . If  $\text{HNO}_3$  will further decrease to 3 ppbv the total time will be  $\sim 5000$  h less than during reference conditions. On the other hand, if in the future  $\text{H}_2\text{O}$  increases and the temperature decreases in the stratosphere, the total time where temperature falls below  $T_{\text{NAT}}$  will increase independent of the  $\text{HNO}_3$  abundance (3, 5 or 7 ppbv) in the stratosphere (Fig. 8). Any  $\text{H}_2\text{O}$  increase of 0.25 ppmv will result in 1500 h more where the temperature along the trajectories will be below  $T_{\text{NAT}}$ . The effect is much stronger when the temperature is decreased by 0.5 K. For each 0.5 K cooling the time will be increased by  $\sim 4000$  h (Fig. 7 and tables in the Supplement).

Temperatures below  $T_{\text{ice}}$  are rarely reached in the Arctic. However, the Arctic winter 2010/11 was exceptionally cold and temperatures below  $T_{\text{ice}}$  were reached along several trajectories. Under typical stratospheric conditions ( $\text{H}_2\text{O} = 5$  ppmv) temperatures were below  $T_{\text{ice}}$  for 571 h (Fig. 7). If the  $\text{H}_2\text{O}$  abundance in the stratosphere is 0.25 ppmv less (thus 4.75 ppmv) then the total time where the temperatures are below  $T_{\text{ice}}$  decreases to 340 h, 231 h less than under the reference stratospheric conditions (Fig. 10 and the Supplement). If the  $\text{H}_2\text{O}$  mixing ratio increases by 0.25 ppmv, from 5 to 5.25 ppmv, temperatures below  $T_{\text{ice}}$  would persist 299 h longer than for reference conditions. If water vapour increases further from 5 to 5.5 or 6 ppmv, the time where temperatures are below  $T_{\text{ice}}$  will increase by 669 and 1728 h, respectively. Thus, the higher the water vapour gets in the stratosphere the stronger the impact of a further increase will be. The same behaviour is found when the temperature in the stratosphere is cooled by 0.5 to 1 K. In the extreme case when  $\text{H}_2\text{O}$  mixing ratios would increase by 1 ppmv and the temperature would decrease by 1 K the total time where temperatures are below  $T_{\text{ice}}$  would increase from 571 to 6789 h, thus by  $\sim 6000$  h which corresponds to an enhancement by a factor of 12.

## Sensitivity of PSCs to $\text{H}_2\text{O}$ and temperature changes

F. Khosrawi et al.

[Title Page](#)[Abstract](#)[Introduction](#)[Conclusions](#)[References](#)[Tables](#)[Figures](#)[Back](#)[Close](#)[Full Screen / Esc](#)[Printer-friendly Version](#)[Interactive Discussion](#)

## 5 H<sub>2</sub>O and temperature (2000–2014)

In order to investigate water vapour variability and/or potential trends in the polar lower stratosphere water vapour and temperature measurements derived from UARS/HALOE, Odin/SMR, Envisat/MIPAS, SCISAT/ACE-FTS, Envisat/SCIAMACHY and Aura/MLS are used. Time series for the time period 2000–2014 are derived from these measurements. Temperature and water vapour in the polar regions at high equivalent latitudes (range 70 to 90° N) were averaged on a monthly basis within the potential temperature range 475–525 K (~ 18–22 km) and 525–825 K (~ 22–28 km). Individual water vapour profiles were first interpolated on a regular grid in terms of potential temperature with a grid resolution of 25 K. Then monthly averages based on all available profiles within the equivalent latitude range 70 to 90° were calculated. Temperature and pressure profiles that were needed for the conversion from the native vertical coordinate system to the potential temperature coordinate system have been taken from the individual satellite data sets.

Anomalies (monthly zonal mean minus a multi-year monthly zonal mean) of the water vapour and temperature time series are derived to separate the relative contributions of cyclic processes of seasonal nature (as e.g. Semi-annual Oscillation (SAO), Quasi-biennial Oscillation (QBO), solar cycles) from the unexplained variability of the monthly mean signal (Jones et al., 2009). Figures 11 and 12 show the time series of the anomaly of the zonally averaged temperature and water vapour for the polar regions and potential temperature ranges 475–525 K (18–22 km) and 525–825 K (22–28 km) for the time period 2000–2014. The temperature time series anomaly was derived from ERA-Interim, Aura/MLS, Envisat/MIPAS and SCISAT/ACE-FTS and the anomaly of water vapour from Odin/SMR, Aura/MLS, Envisat/MIPAS, SCISAT/ACE-FTS, Envisat/SCIAMACHY (note: only shown in Fig. 11) and UARS/HALOE. The time-series have been deseasonalised and offset corrected individually for each satellite data set in order to remove short-term variability (Urban et al., 2012). All satellite instruments show a relatively good agreement in observing the inter-annual variability which shows

### Sensitivity of PSCs to H<sub>2</sub>O and temperature changes

F. Khosrawi et al.

Title Page

Abstract

Introduction

Conclusions

References

Tables

Figures



Back

Close

Full Screen / Esc

Printer-friendly Version

Interactive Discussion



## Sensitivity of PSCs to H<sub>2</sub>O and temperature changes

F. Khosrawi et al.

Title Page

Abstract

Introduction

Conclusions

References

Tables

Figures



Back

Close

Full Screen / Esc

Printer-friendly Version

Interactive Discussion



the accuracy of the different water vapour data sets analysed here. In both potential temperature ranges no clear linear change (trend) in temperature is found in the polar regions. The same holds for stratospheric water vapour. Figure 13 provides a summary of the linear changes in the altitude range between 350 and 1000 K potential temperature based on a regression of Envisat/MIPAS and Aura/MLS observations. Trend estimates were derived with the regression model by von Clarmann et al. (2010) as applied in Stiller et al. (2012) for deriving trends of age of air. The regression model considers an offset, a linear term, periodic variations of 3, 4, 6 and 12 months as well as the QBO in form of Singapore winds at 50 and 30 hPa<sup>3</sup>. In addition the model considers autocorrelation effects and a possible offset between the MIPAS full and reduced resolution data (von Clarmann et al., 2010; Stiller et al., 2012). Even though the two instruments cover slightly different time periods both show consistently no significant linear changes (at the 2  $\sigma$  uncertainty level) except in water vapour slightly above 700 K potential temperature.

However, water vapour and temperature show a clear anti-correlation, e. g. enhanced water vapour mixing ratios occur in cold winters. This is visible in both the 474–525 K (Fig. 14) and the 525–825 K range (see figure in Supplement), as e.g. for the winter 2004/05, 2006/07, 2007/08 and 2010/11. This correlation is quite significant, especially at the lower potential temperature range (475–525 K). This is shown in Fig. 14 where again temperature and water vapour data from Envisat/MIPAS (upper panel) and Aura/MLS (lower panel) observations are considered. The individual data points are averages over the months January, February and March. The correlation coefficients are  $-0.65$  for MIPAS and  $-0.87$  for MLS. This correlation indicates a connection between dynamical processes that influence the polar winter dynamics and enhance (downward and poleward) transport of water vapour. Figure 15 shows the altitude time evolution of water vapour in the polar regions derived from Envisat/MIPAS observations for the time period 2002–2012. Differences in the downward transport of water vapour from year to year are clearly visible during the time period 2002–2012, e.g. reaches

<sup>3</sup><http://www.geo.fu-berlin.de/met/ag/strat/produkte/qbo/index.html>



rupted twice in the last 30 years by sudden drops, one in 2000–2001 (Randel et al., 2006) and another one in 2011–2012 (Urban et al., 2014). Although Hegglin et al. (2014) could not confirm the trend found in the lower stratosphere in the Boulder time series by analysing merged satellite data sets, they found a significant positive trend in the upper stratosphere.

The aforementioned studies were focusing on the tropics which is the entry point for water vapour into the stratosphere as well as on the mid-latitudes. In this study, however, we focus on the polar regions to understand how water vapour and temperature changes in the lower polar stratosphere affect PSC formation and existence. In the satellite data sets applied in this study no trend is observed in the polar lower stratosphere (18–28 km) during the past 15 years, but a significant correlation between cold winters and enhanced water vapour mixing ratios is found. This correlation is quite significant, especially at the lower potential temperature range (475–525 K, correlation coefficient of  $-0.65$  (MIPAS) and  $-0.87$  (MLS), respectively). This correlation indicates a connection between dynamical processes that influence the polar winter dynamics and enhance (downward and poleward) transport of water vapour.

By performing sensitivity studies we, on one hand, investigate what implications water vapour and temperature changes/variability would have on PSC formation and existence. On the other hand this sensitivity study also shows what implications uncertainties in water vapour from measurements and temperature measurements/reanalyses would have on Arctic studies. Gravity waves can affect PSC occurrence and composition in the Arctic and Antarctic McDonald et al. (2009); Alexander et al. (2011, 2013). Temperature perturbation that are caused by gravity waves are usually not represented in meteorological analyses. Further, meteorological analyses tend to have cold or warm biases as was shown by e.g. Manney et al. (1996). PSC formation and existence is quite sensitive to temperature and water vapour changes as well as uncertainties of these. An increase of e.g. 1 ppmv in water vapour and a decrease of 1 K in temperature would significantly alter the estimates of PSC volume and area ( $V_{\text{PSC}}$  and  $A_{\text{PSC}}$ ,

## Sensitivity of PSCs to $\text{H}_2\text{O}$ and temperature changes

F. Khosrawi et al.

Title Page

Abstract

Introduction

Conclusions

References

Tables

Figures



Back

Close

Full Screen / Esc

Printer-friendly Version

Interactive Discussion



respectively) and thus would affect the estimates on e.g. ozone loss and chlorine activation (Manney et al., 2003).

Our sensitivity study was performed on the basis of the 2010/11 winter, which was the coldest Arctic winter in the recent decade. The anomalously strong polar vortex and the atypically long cold period that persisted from mid-December to mid-March led to extensive PSC formation. PSCs were observed by CALIPSO on 47 days during the Arctic winter 2010/11. During the Arctic winter 2009/10, a cold period extended over four weeks, from mid-December to mid-January and PSCs were only observed on 26 days. Thus, if this study would have been performed on the basis of another (warmer) winter less PSC observations would have been served as basis for the trajectory calculations and thus as basis for the statistic. As consequence the total times where the temperature was below  $T_{\text{NAT}}$  or  $T_{\text{ice}}$ , respectively, would have been shorter as for the Arctic winter 2010/11. However, the resulting increase in time due to temperature and water vapour changes can be expected to be similar.

As shown in this study, increases in stratospheric water vapour as well as decreases in stratospheric temperature can prolong PSC formation and existence. An increase of water vapour of 1 ppmv and a decrease of temperature of 1 K increased the times where the temperature is below  $T_{\text{NAT}}$  by 38 %. A much stronger increase in time was found for ice. The increase in time where temperatures were below  $T_{\text{ice}}$  were enhanced by an factor of 12 for an increase of  $\text{H}_2\text{O}$  by 1 ppmv and a temperature decrease of 1 K. Generally, temperatures sufficiently low for ice formation are rarely reached in the Arctic. Therefore, this strong increase in time where temperatures would be below  $T_{\text{ice}}$  would mainly be of importance for very cold, extreme Arctic winters as e.g. the Arctic winter 2010/11. However, if cold Arctic winters will become colder in the future (Rex et al., 2004, 2006), ice formation will also become more common in the Arctic. Thus, changes in stratospheric  $\text{H}_2\text{O}$  mixing ratio and temperature can significantly alter PSC formation and existence and thus the chemistry of the polar stratosphere, as e.g. increasing denitrification and thus ozone loss.

## Sensitivity of PSCs to $\text{H}_2\text{O}$ and temperature changes

F. Khosrawi et al.

[Title Page](#)[Abstract](#)[Introduction](#)[Conclusions](#)[References](#)[Tables](#)[Figures](#)[Back](#)[Close](#)[Full Screen / Esc](#)[Printer-friendly Version](#)[Interactive Discussion](#)

## 7 Conclusions

The Arctic winter 2010/11 was one of the coldest in the last two decades. The 2010/11 winter was characterised by an anomalously strong vortex with an atypically long cold period that was persistent from mid-December to mid-March. During the Arctic winter 2010/11 the strongest denitrification during the recent decade was observed. More than a decade ago it was already suggested that a cooling of stratospheric temperatures by 1 K or an increase of 1 ppmv of stratospheric water vapour could promote denitrification, the removal of  $\text{HNO}_3$  by sedimenting PSC particles.

Based on the 2010/11 winter a sensitivity study was performed to investigate how a change of up to 1 ppmv in water vapour and temperature decrease of up to 1 K (due to a trend or variability) would affect PSC formation and occurrence. Air parcel trajectories were calculated 6 days backward according to PSC observations by CALIPSO. In total 738 trajectories were calculated. On the basis of this trajectory ensemble the increase in time the air parcels would be exposed to temperatures below  $T_{\text{NAT}}$  or  $T_{\text{ice}}$  along the trajectories was calculated. Measurements from several different satellites derived for the 15 year period 2000–2014 were used together with temperatures from ECMWF to investigate water vapour trends and variability in the polar stratosphere. So far trend studies on stratospheric water vapour have focused on the tropics and mid-latitudes. Here, for the first time such an analyses has been performed for the polar stratosphere.

Our sensitivity studies based on air parcel trajectories confirm that PSC formation is quite sensitive to water vapour and temperature changes. Increased  $\text{H}_2\text{O}$  (and further cooling of the stratosphere) would increase the potential for PSC formation and prolong PSC existence and thus the chemistry of the polar stratosphere, as e.g. increasing denitrification and thus ozone loss. On the other hand an increase in temperature and a decrease in water vapour will reduce PSC formation and existence. The previously reported abrupt decrease in lower stratospheric water vapour in the tropical tropopause region (by about 1 ppmv) in 2000–2001 can also be observed with a lesser extent and a few years delay in the Arctic. This delay is caused by atmospheric transport

### Sensitivity of PSCs to $\text{H}_2\text{O}$ and temperature changes

F. Khosrawi et al.

Title Page

Abstract

Introduction

Conclusions

References

Tables

Figures



Back

Close

Full Screen / Esc

Printer-friendly Version

Interactive Discussion





The Supplement related to this article is available online at  
doi:10.5194/acpd-15-17743-2015-supplement.

*Acknowledgements.* We are grateful to the European Space Agency (ESA) for providing Odin/SMR data. Odin is a Swedish-led satellite project jointly funded by the Swedish National Space Board (SNSB), the Canadian Space Agency (SCA), the National Technology Agency of Finland (Tekes) and the Centre National d'Etudes Spatiales (CNES) in France. SCISAT/ACE is a Canadian led mission mainly supported by the CSA and National Sciences and Engineering Research Council of Canada (NSERC). Provision of MIPAS level-1b data by ESA is gratefully acknowledged. We also would like to thank the MLS team for providing their data. MLS data were obtained from the NASA Goddard Earth Sciences Data and Information Center. The SCIAMACHY limb water vapour data V3.01 are a result of the DFG Research Unit "Stratospheric Change and its role for Climate Prediction (SHARP)" and the ESA Project SPIN (ESA SPARC Initiative) and were partly calculated using resources of the German HLRN (High-Performance Computer Center North). We also would like to thank M. Hervig for providing a program to calculate the NAT existence temperature. We gratefully acknowledge the NOAA Air Resources Laboratory (ARL) for the provision of the HYSPLIT READY website (<http://ready.arl.noaa.gov/HYSPLIT.php>). This study was performed in the frame of the FP7 project RECONCILE (Grant number: RECONCILE-226365-FP7-ENV-2008-1). We are also grateful to SNSB for funding F. Khosrawi (2012–2013).

The article processing charges for this open-access publication were covered by a Research Centre of the Helmholtz Association.

## References

Achtert, P., Khosrawi, F., Blum, U., and Fricke, K.-H.: Investigation of polar stratospheric clouds in January 2008 by means of ground-based and space-borne lidar measurements and microphysical box model simulations, *J. Geophys. Res.*, 116, D07201, doi:10.1029/2010JD014803, 2011. 17758

ACPD

15, 17743–17796, 2015

## Sensitivity of PSCs to H<sub>2</sub>O and temperature changes

F. Khosrawi et al.

Title Page

Abstract

Introduction

Conclusions

References

Tables

Figures



Back

Close

Full Screen / Esc

Printer-friendly Version

Interactive Discussion



**Sensitivity of PSCs to H<sub>2</sub>O and temperature changes**

F. Khosrawi et al.

Title Page

Abstract

Introduction

Conclusions

References

Tables

Figures



Back

Close

Full Screen / Esc

Printer-friendly Version

Interactive Discussion



Alexander, S. P., Klekociuk, A. R., Pitts, M. C., McDonald, A. J., and Arevalo-Torres, A.: The effect of orographic gravity waves on Antarctic polar stratospheric cloud occurrence and composition, *J. Geophys. Res.*, 116, D06109, doi:10.1029/2010JD015184, 2011. 17764

Alexander, S. P., Klekociuk, A. R., McDonald, A. J., and Pitts, M. C.: Quantifying the role of orographic waves on polar stratospheric cloud occurrence in the Antarctic and the Arctic, *J. Geophys. Res.*, 118, 11493–11507, doi:10.1002/2013JD020122, 2013. 17764

Arnone, E., Castelli, E., Papandrea, E., Carlotti, M., and Dinelli, B. M.: Extreme ozone depletion in the 2010–2011 Arctic winter stratosphere as observed by MIPAS/ENVISAT using a 2-D tomographic approach, *Atmos. Chem. Phys.*, 12, 9149–9165, doi:10.5194/acp-12-9149-2012, 2012. 17748, 17754, 17755

Austin, J., Butchart, N., and Shine, K. P.: Possibility of an Arctic ozone hole in a doubled-CO<sub>2</sub> climate, *Nature*, 360, 221–225, 1992. 17747

Bernath, P. F., McElroy, C. T., Abrams, M. C., Boone, C. D., Butler, M., Camy-Peyret, C., Carleer, M., Clerbaux, C., Coheur, P.-F., Colin, R., DeCola, P., DeMazière, M., Drummond, J. R., Dufour, D., Evans, W. F. J., Fast, H., Fussen, D., Gilbert, K., Jennings, D. E., Llewellyn, E. J., Lowe, R. P., Mahieu, E., McConnell, J. C., McHugh, M., McLeod, S. D., Michaud, R., Midwinter, C., Nassar, R., Nichitiu, F., Nowlan, C., Rinsland, C. P., Rochon, Y. J., Rowlands, N., Semeniuk, K., Simon, P., Skelton, R., Sloan, J. J., Soucy, M.-A., Strong, K., Tremblay, P., Turnbull, D., Walker, K. A., Walkty, I., Wardle, D. A., Wehrle, V., Zander, R., and Zou, J.: Atmospheric Chemistry Experiment (ACE): mission overview, *Geophys. Res. Lett.*, 32, L15S01, doi:10.1029/2005GL022368, 2005. 17752

Bogdan, A., Molina, M. J., Kulmala, M., MacKenzie, A. R., and Laaksonen, A.: Study of finely divided aqueous systems as an aid to understanding the formation mechanism of polar stratospheric clouds: case of HNO<sub>3</sub>/H<sub>2</sub>O and H<sub>2</sub>SO<sub>4</sub>/H<sub>2</sub>O system, *J. Geophys. Res.*, 4302, doi:10.1029/2002JD002605, 2003. 17746

Boone, C. D., Nassar, R., Walker, K. A., Rochon, Y., McLeod, S. D., Rinsland, C. P., and Bernath, P. F.: Retrievals for the atmospheric chemistry experiment Fourier transform spectrometer, *Appl. Optics*, 44, 7218–7231, 2005. 17752

Bovensmann, H., Burrows, J. P., Buchwitz, M., Frerick, J., Noël, S., Rozanov, V. V., Chance, K. V., and Goede, A. P. H.: SCIAMACHY: mission objectives and measurement modes, *J. Atmos. Sci.*, 56, 127–150, 1999. 17751

## Sensitivity of PSCs to H<sub>2</sub>O and temperature changes

F. Khosrawi et al.

Title Page

Abstract

Introduction

Conclusions

References

Tables

Figures



Back

Close

Full Screen / Esc

Printer-friendly Version

Interactive Discussion



Burrows, J. P., Hölzle, E., Goede, A. P. H., Visser, H., and Fricke, W.: SCIAMACHY – scanning imaging absorption spectrometer for atmospheric cartography, *Acta Astronaut.*, 35, 445–451, 1995. 17751

Carlsaw, K. S., Luo, B. P., Clegg, S. L., Peter, T., Brimblecombe, P., and Crutzen, P. J.: Stratospheric aerosol growth and HNO<sub>3</sub> gas phase depletion from coupled HNO<sub>3</sub> and water uptake by liquid particles, *Geophys. Res. Lett.*, 21, 2479–2482, 1994. 17746

Dessler, A. E., Schoeberl, M. R., Wang, T., Davis, S. M., Rosenlof, K. H., and Vernier, J.-P.: Variations of stratospheric water vapour over the past three decades, *J. Geophys. Res.*, 119, 12588–12598, doi:10.1002/2014JD021712, 2014. 17747

Engel, I., Luo, B. P., Khaykin, S. M., Wienhold, F. G., Vömel, H., Kivi, R., Hoyle, C. R., Grooß, J.-U., Pitts, M. C., and Peter, T.: Arctic stratospheric dehydration Part 2: Microphysical modeling, *Atmos. Chem. Phys.*, 14, 3231–3246, doi:10.5194/acp-14-3231-2014, 2014. 17747

Eyring, V., Cionni, I., Lamarque, J. F., Akiyoshi, H., Bodeker, G. E., Charlton-Perez, A. J., Frith, S. M., Gettelman, A., Kinnison, D. E., Nakamura, T., Oman, L. D., Pawson, S., and Yamashita, Y.: Sensitivity of 21st century stratospheric ozone to greenhouse gas scenarios, *Geophys. Res. Lett.*, 37, L16807, doi:10.1029/2010GL044443, 2010. 17747

Fischer, H. and Oelhaf, H.: Remote sensing of vertical profiles of atmospheric trace constituents with MIPAS limb-emission spectrometers, *Appl. Optics*, 35, 2787–2796, 1996. 17751

Fischer, H., Birk, M., Blom, C., Carli, B., Carlotti, M., von Clarmann, T., Delbouille, L., Dudhia, A., Ehhalt, D., Endemann, M., Flaud, J. M., Gessner, R., Kleinert, A., Koopman, R., Langen, J., López-Puertas, M., Mosner, P., Nett, H., Oelhaf, H., Perron, G., Remedios, J., Ridolfi, M., Stiller, G., and Zander, R.: MIPAS: an instrument for atmospheric and climate research, *Atmos. Chem. Phys.*, 8, 2151–2188, doi:10.5194/acp-8-2151-2008, 2008. 17751

Frisk, U., Gastrom, M., Ala-Laurinaho, J., Andersson, S., Berges, J. C., Chabaud, J. P., Dahlgren, M., Emrich, A., Florin, G., Fredrixon, M., Gaier, T., Haas, R., Hjalmarsson, T. H. A., Jakobsson, B., Jukkala, P., Kildal, P. S., Kollberg, E., Lecacheux, J. L. A., Lehtikoinen, P., Lehto, A., Mallat, J., Marty, C., Michet, D., Narbonne, J., Nexon, M., Olberg, M., Olofsson, A. O. H., Olofsson, G., Origne, A., Petersson, M., Piirone, P., Pouliquen, D., Ristorcelli, I., Rosolen, C., Rouaix, G., Raisanen, A. V., Serra, G., Sjöberg, F., Stenmark, L., Torchinsky, S., Tuovinen, J., Ullberg, C., Vinterhav, E., Wadefalk, N., Zirath, H., Zimmermann, P., and Zimmermann, R.: The Odin satellite: I. Radiometer design and test, *Astron. Astrophys.*, 403, 27–34, 2003. 17750

**Sensitivity of PSCs to H<sub>2</sub>O and temperature changes**

F. Khosrawi et al.

Title Page

Abstract

Introduction

Conclusions

References

Tables

Figures



Back

Close

Full Screen / Esc

Printer-friendly Version

Interactive Discussion



Fueglistaler, S., Buss, S., Luo, B. P., Wernli, H., Flentje, H., Hostetler, C. A., Poole, L. R., Carslaw, K. S., and Peter, Th.: Detailed modeling of mountain wave PSCs, *Atmos. Chem. Phys.*, 3, 697–712, doi:10.5194/acp-3-697-2003, 2003. 17746

5 Guttelman, A., Hegglin, M. I., Son, S., Kim, J., Fujiwara, M., Birner, T., Kremser, S., Rex, M., Anel, J. A., Austin, H. A. J., Bekki, S., Braesicke, P., Brühl, C., Butchart, N., Chipperfield, M., Dameris, M., Dhomse, S., Garny, H., Hardiman, S. C., Jöckel, P., Kinnison, D. E., Lamarque, J. F., Mancini, E., Marchand, M., Michou, M., Morgenstern, O., Pawson, S., Pitari, G., Plummer, D., Pyle, J. A., Rozanov, E., Scinocca, J., Shepherd, T. G., Shibata, K., Smale, D., Teysseèdre, H., and Tian, W.: Multimodel assessment of the upper troposphere and lower stratosphere: tropics and global trends, *J. Geophys. Res.*, 115, D00M08, doi:10.1029/2009JD013638, 2010. 17747

10 Gottwald, M., Bovensmann, H., Lichtenberg, G., Noel, S., von Barmen, A., Slijkhuis, S., Piders, A., Hoogeveen, R., von Savigny, C., Buchwitz, M., Kokhanovsky, A., Richter, A., Rozanov, A., Holzer-Popp, T., Bramstedt, K., Lambert, J.-C., Skupin, J., Wittrock, F., Schrijver, H., and Burrows, J.: *SCIAMACHY, Monitoring the Changing Earth's Atmosphere*, Springer, Dordrecht, Heidelberg, London, New York, 2006. 17752

15 Hanson, D. R. and Mauersberger, K.: Laboratory studies of the nitric acid trihydrate: implications for the south polar stratosphere, *Geophys. Res. Lett.*, 15, 855–858, 1988. 17757

20 Harris, J. E., Russell, J. M., Tuck, A. F., Gordely, L. L., Purcell, P., Stone, K., Bevilacqua, R. M., Gunson, M., Nedoluha, G., and Traub, W. A.: Validation of measurements of water vapour from the Halogen Occultation Experiment (HALOE), *J. Geophys. Res.*, 101, 10205–10216, 1996. 17753

25 Hegglin, M. I., Tegtmeier, S., Anderson, J., Froidevaux, L., Fuller, R., Funke, B., Jones, A., Lingenfelter, G., Lumpe, J., Pendlebury, D., Remsberg, E., Rozanov, A., Toohey, M., Urban, J., von Clarmann, T., Walker, K. A., Wang, R., and Weigel, K.: SPARC data initiative: comparison of water vapor climatologies from international satellite limb sounders, *J. Geophys. Res.*, 118, 11824–11846, doi:10.1002/jgrd.50752, 2013. 17749

30 Hegglin, M. I., Plummer, D. A., Shepherd, T. G., Scinocca, J. F., Anderson, J., Froidevaux, L., Funke, B., Hurst, D., Rozanov, A., Urban, J., von Clarmann, T., Walker, K. A., Wang, H. J., Tegtmeier, S., and Weigel, K.: Vertical structure of stratospheric water vapour trends derived from merged satellite data, *Nat. Geosci.*, 7, 768–776, doi:10.1038/ngeo2236, 2014. 17747, 17764

**Sensitivity of PSCs to  
H<sub>2</sub>O and temperature  
changes**

F. Khosrawi et al.

Title Page

Abstract

Introduction

Conclusions

References

Tables

Figures



Back

Close

Full Screen / Esc

Printer-friendly Version

Interactive Discussion



- Hommel, R., Eichmann, K.-U., Aschmann, J., Bramstedt, K., Weber, M., von Savigny, C., Richter, A., Rozanov, A., Wittrock, F., Khosrawi, F., Bauer, R., and Burrows, J. P.: Chemical ozone loss and ozone mini-hole event during the Arctic winter 2010/2011 as observed by SCIAMACHY and GOME-2, *Atmos. Chem. Phys.*, 14, 3247–3276, doi:10.5194/acp-14-3247-2014, 2014. 17748, 17755
- Höpfner, M., Larsen, N., Spang, R., Luo, B. P., Ma, J., Svendsen, S. H., Eckermann, S. D., Knudsen, B., Massoli, P., Cairo, F., Stiller, G., v. Clarmann, T., and Fischer, H.: MIPAS detects Antarctic stratospheric belt of NAT PSCs caused by mountain waves, *Atmos. Chem. Phys.*, 6, 1221–1230, doi:10.5194/acp-6-1221-2006, 2006. 17746
- Höpfner, M., Pitts, M. C., and Poole, L. R.: Comparison between CALIPSO and MIPAS observations of polar stratospheric clouds, *J. Geophys. Res.*, 114, D00H05, doi:10.1029/2009JD012114, 2009. 17755
- Hoyle, C. R., Engel, I., Luo, B. P., Pitts, M. C., Poole, L. R., Groß, J.-U., and Peter, T.: Heterogeneous formation of polar stratospheric clouds – Part 1: Nucleation of nitric acid trihydrate (NAT), *Atmos. Chem. Phys.*, 13, 9577–9595, doi:10.5194/acp-13-9577-2013, 2013. 17746, 17747
- Hurst, D. F., Oltmans, S. J., Vömel, H., Rosenlof, K. H., Davies, S. M., Ray, E. A., Hall, E. G., and Jordan, A. F.: Stratospheric water vapour trends over Boulder, Colorado: analysis of 30 year Boulder record, *J. Geophys. Res.*, 116, D02306, doi:10.1029/2010JD015065, 2011. 17747, 17763
- Hurst, D. F., Lambert, A., Read, W. G., Davis, S. M., Rosenlof, K. H., Hall, E. G., Jordan, A. F., and Oltmans, S. J.: Validation of aura microwave limb sounder stratospheric water vapor measurements by the NOAA frost point hygrometer, *J. Geophys. Res.*, 119, 1612–1625, doi:10.1002/2013JD020757, 2014. 17750
- Hurwitz, M. M., Newman, P. A., and Garfinkel, C. I.: The Arctic vortex in March 2011: a dynamical perspective, *Atmos. Chem. Phys.*, 11, 11447–11453, doi:10.5194/acp-11-11447-2011, 2011. 17755
- Jones, A., Urban, J., Murtagh, D. P., Eriksson, P., Brohede, S., Haley, C., Degenstein, D., Bourassa, A., von Savigny, C., Sonkaew, T., Rozanov, A., Bovensmann, H., and Burrows, J.: Evolution of stratospheric ozone and water vapour time series studied with satellite measurements, *Atmos. Chem. Phys.*, 9, 6055–6075, doi:10.5194/acp-9-6055-2009, 2009. 17761
- Khosrawi, F., Urban, J., Pitts, M. C., Voelger, P., Achtert, P., Kaphlanov, M., Santee, M. L., Manney, G. L., Murtagh, D., and Fricke, K.-H.: Denitrification and polar stratospheric

**Sensitivity of PSCs to H<sub>2</sub>O and temperature changes**

F. Khosrawi et al.

[Title Page](#)[Abstract](#)[Introduction](#)[Conclusions](#)[References](#)[Tables](#)[Figures](#)[Back](#)[Close](#)[Full Screen / Esc](#)[Printer-friendly Version](#)[Interactive Discussion](#)

cloud formation during the Arctic winter 2009/2010, *Atmos. Chem. Phys.*, 11, 8471–8487, doi:10.5194/acp-11-8471-2011, 2011. 17748, 17758

Khosrawi, F., Urban, J., Pitts, M. C., Voelger, P., Achtert, P., Santee, M. L., Manney, G. L., and Murtagh, D.: Denitrification and polar stratospheric cloud formation during the Arctic winter 2009/2010 and 2010/2011 in comparison, in: *Proceedings of the ESA Atmospheric Science Conference: Advances in Atmospheric Science and Application*, 18–22 June 2012, Brugge, Belgium, edited by: Ouwehand, L., ESA-SP-708, Eur. Space Agency Spec. Publ., ISBN/ISSN:978-92-9092-272-8, 2012. 17748, 17754

Koop, T., Biermann, U. M., Raber, W., Luo, B. P., Crutzen, P. J., and Peter, T.: Do stratospheric aerosol droplets freeze above the ice frost point?, *Geophys. Res. Lett.*, 22, 917–920, 1995. 17746

Kuttippurath, J., Godin-Beekmann, S., Lefèvre, F., Nikulin, G., Santee, M. L., and Froidevaux, L.: Record-breaking ozone loss in the Arctic winter 2010/2011: comparison with 1996/1997, *Atmos. Chem. Phys.*, 12, 7073–7085, doi:10.5194/acp-12-7073-2012, 2012. 17748, 17754, 17755

Labitzke, K. and Kunze, M.: On the remarkable Arctic winter in 2008/2009, *J. Geophys. Res.*, 114, D00I02, doi:10.1029/2009JD012273, 2009. 17763

Lambert, A., Read, W. G., Livesey, N. J., Santee, M. L., Manney, G. L., Froidevaux, L., Wu, D. L., Schwartz, M. J., Pumphrey, H. C., Jimenez, C., Nedoluha, G. E., Cofield, R. E., Cuddy, D. T., Daffer, W. H., Drouin, B. J., Fuller, R. A., Jarnot, R. F., Knosp, B. W., Pickett, H. M., Perrun, V. S., Snyder, W. V., Stek, P. C., Thurstans, R. P., Wagner, P. A., Waters, J. W., Jucks, K. W., Toon, G. C., Stachnik, R. A., Bernath, P. F., Boone, C. D., Walker, K. A., Urban, J., Murtagh, D., Elkins, J. W., and Atlas, E.: Validation of the aura microwave limb sounder middle atmosphere water vapor and nitrous oxide measurements, *J. Geophys. Res.*, 112, D24S36, doi:10.1029/2007JD008724, 2007. 17750

Llewellyn, E. J., Lloyd, N. D., Degenstein, D. A., Gattinger, R. L., Petelina, S. V., Bourassa, A. E., Wiensz, J. T., Ivanov, E. V., Dade, I. C. M., Solheim, B. H., Connell, J. C. M., Haley, J. C., von Savigny, C., et al.: The OSIRIS instrument on the Odin spacecraft, *Can. J. Phys.*, 82, 411–422, 2004. 17750

Luo, B. P., Voigt, C., Fueglistaler, S., and Peter, T.: Extreme NAT supersaturations in mountain wave ice PSCs: a clue to NAT formation, *J. Geophys. Res.*, 108, 4441, doi:10.1029/2002JD003104, 2003. 17746

## Sensitivity of PSCs to H<sub>2</sub>O and temperature changes

F. Khosrawi et al.

Title Page

Abstract

Introduction

Conclusions

References

Tables

Figures



Back

Close

Full Screen / Esc

Printer-friendly Version

Interactive Discussion



- Manney, G. L., Swinbank, R., Massie, S. T. S., Gelman, M. E., Miller, A. J., Nagatani, R., O'Neill, A., and Zurek, R. W.: Comparison of UK Meteorological Office and US National Meteorological Center stratospheric analyses during northern and southern winter, *J. Geophys. Res.*, 101, 10311–10334, doi:10.1029/95JD03350, 1996. 17764
- 5 Manney, G. L., Sabutis, J. L., Pawson, S., Santee, M. L., Naujokat, B., Swinbank, R., Gelman, M. E., and Ebisuzaki, W.: Lower stratospheric temperature differences between meteorological analyses in two cold winters and their impact on polar processing studies, *J. Geophys. Res.*, 108, 8328, doi:10.1029/2001JD001149, 2003. 17765
- Manney, G. L., Santee, L., M., Rex, M., Livesey, N. L., Pitts, M. C., Veefkind, P., Nash, E. R., Woltmann, I., Lehmann, R., Froidevaux, L., Poole, L. R., Schoeberl, M. R., Haffner, D. P., Davies, J., Dorokhov, V., Gernandt, H., Johnson, B., Kivi, R., Kyrö, E., Larsen, N., Levelt, P. F., Makshtas, A., McElroy, C. T., Nakajima, H., Concepcion Parrondo, M., Tarasick, D. W., von der Gathen, P., Walker, K. A., and Zinoviev, N. S.: Unprecedented Arctic ozone loss in 2011, *Nature*, 478, 469–475, doi:10.1038/nature10556, 2011. 17748, 17754, 17755
- 15 Marti, J. and Mauersberger, K.: A survey and new measurements of ice vapor pressure temperatures between 170 and 250 K, *Geophys. Res. Lett.*, 20, 363–366, 1993. 17757
- McDonald, A. J., George, S. E., and Woollands, R. M.: Can gravity waves significantly impact PSC occurrence in the Antarctic?, *Atmos. Chem. Phys.*, 9, 8825–8840, doi:10.5194/acp-9-8825-2009, 2009. 17764
- 20 Milz, M., Clarmann, T. v., Bernath, P., Boone, C., Buehler, S. A., Chauhan, S., Deuber, B., Feist, D. G., Funke, B., Glatthor, N., Grabowski, U., Griesfeller, A., Haefele, A., Höpfner, M., Kämpfer, N., Kellmann, S., Linden, A., Müller, S., Nakajima, H., Oelhaf, H., Remsberg, E., Rohs, S., Russell III, J. M., Schiller, C., Stiller, G. P., Sugita, T., Tanaka, T., Vömel, H., Walker, K., Wetzell, G., Yokota, T., Yushkov, V., and Zhang, G.: Validation of water vapour profiles (version 13) retrieved by the IMK/IAA scientific retrieval processor based on full resolution spectra measured by MIPAS on board Envisat, *Atmos. Meas. Tech.*, 2, 379–399, doi:10.5194/amt-2-379-2009, 2009. 17751
- 25 Murtagh, D., Frisk, U., Merino, F., Ridal, M., Jonsson, A., Stegman, J., Witt, G., Eriksson, P., Jimenez, C., Megie, G., de la Noe, J., Ricaud, P., Baron, P., Pardo, J. R., Hauchcorne, A., Llewellyn, E. J., Degenstein, D. A., Gattinger, R. L., Lloyd, N. D., Evans, W. F. J., McDade, I. C., Haley, C. S., Sioris, C., von Savigny, C., Solheim, B. H., McConnell, J. C., Strong, K., Richardson, E. H., Leppelmeier, G. W., Kyrola, E., Auvinen, H., and Oikarinen, L.: An overview of the Odin atmospheric mission, *Can. J. Phys.*, 80, 309–319, 2002. 17750
- 30

## Sensitivity of PSCs to H<sub>2</sub>O and temperature changes

F. Khosrawi et al.

[Title Page](#)
[Abstract](#)
[Introduction](#)
[Conclusions](#)
[References](#)
[Tables](#)
[Figures](#)




[Back](#)
[Close](#)
[Full Screen / Esc](#)
[Printer-friendly Version](#)
[Interactive Discussion](#)


- Orsolini, Y. J., Urban, J., Murtagh, D. P., Lossow, S., and Limpasuvan, V.: Descent from the polar mesosphere and anomalously high stratopause observed in 8 years of water vapor and temperature satellite observations by the Odin Sub-Millimeter Radiometer, *J. Geophys. Res.*, 115, D12305, doi:10.1029/2009JD013501, 2010. 17763
- 5 Pitts, M. C., Thomason, L. W., Poole, L. R., and Winker, D. M.: Characterization of Polar Stratospheric Clouds with spaceborne lidar: CALIPSO and the 2006 Antarctic season, *Atmos. Chem. Phys.*, 7, 5207–5228, doi:10.5194/acp-7-5207-2007, 2007. 17753
- Pitts, M. C., Poole, L. R., and Thomason, L. W.: CALIPSO polar stratospheric cloud observations: second-generation detection algorithm and composition discrimination, *Atmos. Chem. Phys.*, 9, 7577–7589, doi:10.5194/acp-9-7577-2009, 2009. 17753
- 10 Pitts, M. C., Poole, L. R., Dörnbrack, A., and Thomason, L. W.: The 2009–2010 Arctic polar stratospheric cloud season: a CALIPSO perspective, *Atmos. Chem. Phys.*, 11, 2161–2177, doi:10.5194/acp-11-2161-2011, 2011. 17746, 17754
- Randel, W. J., Wu, F., Vömel, H., Nedoluha, G. E., and Forster, P.: Decreases in stratospheric water vapor after 2001: links to changes in the tropical tropopause and the Brewer–Dobson circulation, *J. Geophys. Res.*, 111, D12312, doi:10.1029/2005JD006744, 2006. 17763, 17764
- 15 Rex, M., Salawitch, R. J., Deckelmann, H., von der Gathen, P., Harris, N. P., Chipperfield, M. P., and Naujokat, B.: Arctic ozone loss and climate change, *Geophys. Res. Lett.*, 31, L04116, doi:10.1029/2003GL018844, 2004. 17765
- Rex, M., Salawitch, R. J., Deckelmann, H., von der Gathen, P., Harris, N. P., Chipperfield, M. P., Naujokat, B., Reimer, E., Allaart, M., Andersen, S. B., Bevilacqua, R., Braathen, G. O., Claude, H., Davies, J., De Backer, H., Dier, H., Dorokhov, V., Fast, H., Gerding, M., Godin-Beekmann, S., Hoppel, K., Johnson, B., Kyrö, E., Litynska, Z., Moore, D., Nakane, H., Par-  
rondo, M. C., Rislely Jr., A. D., Skrivanova, P., Stubi, R., Viatte, P., Yushkov, V., and Zere-  
fos, C.: Arctic winter 2005: implications for stratospheric ozone loss and climate change, *Geophys. Res. Lett.*, 33, L23808, doi:10.1029/2006GL026731, 2006. 17765
- 25 Rosenlof, K. H., Oltmans, S. J., Kley, D., Russell, J. M., Chiou, E. W., Chu, W. P., Johnson, D. G., Kelly, K. K., Michelsen, H. A., Nedoluha, G. E., Remsberg, E. E., Toon, G. C., and McCormick, M. P.: Stratospheric water vapor increases over the past half-century, *Geophys. Res. Lett.*, 28, 1195–1198, doi:10.1029/2000GL012502, 2001. 17763
- 30 Rozanov, A., Weigel, K., Bovensmann, H., Dhomse, S., Eichmann, K.-U., Kivi, R., Rozanov, V., Vömel, H., Weber, M., and Burrows, J. P.: Retrieval of water vapor vertical distributions in

**Sensitivity of PSCs to H<sub>2</sub>O and temperature changes**

F. Khosrawi et al.

Title Page

Abstract

Introduction

Conclusions

References

Tables

Figures



Back

Close

Full Screen / Esc

Printer-friendly Version

Interactive Discussion



the upper troposphere and the lower stratosphere from SCIAMACHY limb measurements, Atmos. Meas. Tech., 4, 933–954, doi:10.5194/amt-4-933-2011, 2011. 17752

Russell, J. M., Gordley, L. L., Park, J. H., Drayson, S. R., Tuck, A. F., Harries, J. E., Ciccerone, R. J., Crutzen, P. J., and Frederick, J. E.: The halogen occultation experiment, J. Geophys. Res., 98, 10777–10797, 1993. 17753

Santee, M. L., Read, W. G., Waters, J. W., Froidevaux, L., Manney, G. L., Flower, D. A., Jarnot, R. F., Harwood, R. S., and Peckham, G. E.: Interhemispheric differences in polar stratospheric HNO<sub>3</sub>, H<sub>2</sub>O, ClO, and O<sub>3</sub>, Science, 267, 849–852, 1995. 17748

Scherer, M., Vömel, H., Fueglistaler, S., Oltmans, S. J., and Staehelin, J.: Trends and variability of midlatitude stratospheric water vapour deduced from the re-evaluated Boulder balloon series and HALOE, Atmos. Chem. Phys., 8, 1391–1402, doi:10.5194/acp-8-1391-2008, 2008. 17747, 17763

Shindell, D. T., Rind, D., and Lonergan, P.: Increased polar stratospheric ozone losses and delayed eventual recovery owing to increasing greenhouse-gas concentrations, Nature, 392, 589–592, 1998. 17747

Sinnhuber, B.-M., Stiller, G., Ruhnke, R., von Clarmann, T., and Kellmann, S.: Arctic winter 2010/2011 at the brink of an ozone hole, Geophys. Res. Lett., 38, L24814, doi:10.1029/2011GL049784, 2011. 17748, 17754, 17755

Solomon, S., Rosenlof, K. H., Portmann, R. W., Daniel, J. S., Davis, S. M., Sanford, T. J., and Plattner, G.-K.: Contributions of stratospheric water vapor to decadal changes in the rate of global warming, Science, 327, 1219–1223, doi:10.1126/science.1182488, 2010. 17763

SPARC CCMVal: SPARC Report on the Evaluation of Chemistry-Climate Models, edited by: Eyring, V., Shepherd, T. G., and Waugh, D. W., SPARC Report No. 5, WCRP-132, WMO/TD-No. 1526, 2010. 17747

Stiller, G. P., von Clarmann, T., Haenel, F., Funke, B., Glatthor, N., Grabowski, U., Kellmann, S., Kiefer, M., Linden, A., Lossow, S., and López-Puertas, M.: Observed temporal evolution of global mean age of stratospheric air for the 2002 to 2010 period, Atmos. Chem. Phys., 12, 3311–3331, doi:10.5194/acp-12-3311-2012, 2012. 17762, 17763

Tabazadeh, A., Santee, M. L., Danilin, M. Y., Pumphrey, H. C., Newman, P. A., Hamill, P. J., and Mergenthaler, J. L.: Quantifying denitrification and its effect on ozone recovery, Science, 288, 1407–1411, 2000. 17748

Urban, J.: Tropical ascent of lower stratospheric air analysed using measurements of the Odin Sub-Millimetre Radiometer, in: Proc. Reunion Island Int. Symp. Tropical Stratosphere

Sensitivity of PSCs to H<sub>2</sub>O and temperature changes

F. Khosrawi et al.

Title Page

Abstract

Introduction

Conclusions

References

Tables

Figures



Back

Close

Full Screen / Esc

Printer-friendly Version

Interactive Discussion



Upper Troposphere, 5–9 November 2007, St. Gilles, Reunion Island, France, edited by: Bencherif, H., Universite de la Reunion, 2008. 17750

Urban, J., Lautié, N., Le Flochmoën, E., Jiménez, C., Eriksson, P., De La Noë, J., Dupuy, E., Ekström, M., El Amraoui, L., Frisk, U., Murtagh, D., Olberg, M., and Ricaud, P.: Odin/SMR limb observations of stratospheric trace gases: level 2 processing of ClO, N<sub>2</sub>O, HNO<sub>3</sub>, and O<sub>3</sub>, *J. Geophys. Res.*, 110, D14307, doi:10.1029/2004JD005741, 2005a. 17750

Urban, J., Lautié, N., Le Flochmoën, E., Jiménez, C., Eriksson, P., De La Noë, J., Dupuy, E., El Amraoui, L., Frisk, U., Jégou, F., Murtagh, D., Olberg, M., Ricaud, P., Camy-Peyret, C., Dufour, G., Payan, S., Huret, N., Pirre, M., Robinson, A. D., Harris, N. R. P., Bremer, H., Kleinböhl, A., Küllmann, K., Künzi, K., Kuttipurath, J., Ejiri, M. K., Nakajima, H., Sasano, Y., Sugita, T., Yokota, T., Piccolo, C., Raspollini, P., and Ridolfi, M.: Odin/SMR limb observations of stratospheric trace gases: validation of N<sub>2</sub>O, *J. Geophys. Res.*, 110, D09301, doi:10.1029/2004JD005394, 2005b. 17750

Urban, J., Lautie, N., Murtagh, D., Eriksson, P., Kasai, Y., Lossow, S., Dupuy, E., de la Noe, J., Frisk, U., Olberg, M., Flochmoen, E. L., and Ricaud, P.: Global observations of middle atmospheric water vapour by the Odin satellite: an overview, *Planet. Space Sci.*, 55, 1093–1102, 2007. 17750

Urban, J., Murtagh, D. P., Stiller, G., and Walker, K. A.: Evolution and variability of water vapour in the tropical tropopause and lower stratosphere region derived from satellite measurements, in: *Proceedings of the ESA Atmospheric Science Conference: Atmospheric Science and Applications*, 18–22 June 2012, Brugge, Belgium, edited by: Ouwehand, L., ESA-SP-708, Eur. Space Agency Spec. Publ., ISBN/ISSN:978-92-9092-272-8, 2012. 17750, 17761, 17763

Urban, J., Lossow, S., Stiller, G., and Read, W.: Another drop in water vapour, *EOS*, 95, 245–252, 2014. 17764

Voigt, C., Schlager, H., Luo, B. P., Dörnbrack, A., Roiger, A., Stock, P., Curtius, J., Vössing, H., Borrmann, S., Davies, S., Konopka, P., Schiller, C., Shur, G., and Peter, T.: Nitric Acid Trihydrate (NAT) formation at low NAT supersaturation in Polar Stratospheric Clouds (PSCs), *Atmos. Chem. Phys.*, 5, 1371–1380, doi:10.5194/acp-5-1371-2005, 2005. 17746

von Clarmann, T., Höpfner, M., Kellmann, S., Linden, A., Chauhan, S., Funke, B., Grabowski, U., Glatthor, N., Kiefer, M., Schieferdecker, T., Stiller, G. P., and Versick, S.: Retrieval of temperature, H<sub>2</sub>O, O<sub>3</sub>, HNO<sub>3</sub>, CH<sub>4</sub>, N<sub>2</sub>O, ClONO<sub>2</sub> and ClO from MIPAS reduced resolution nominal

## Sensitivity of PSCs to H<sub>2</sub>O and temperature changes

F. Khosrawi et al.

Title Page

Abstract

Introduction

Conclusions

References

Tables

Figures



Back

Close

Full Screen / Esc

Printer-friendly Version

Interactive Discussion



mode limb emission measurements, *Atmos. Meas. Tech.*, 2, 159–175, doi:10.5194/amt-2-159-2009, 2009. 17751

von Clarmann, T., Stiller, G., Grabowski, U., Eckert, E., and Orphal, J.: Technical Note: Trend estimation from irregularly sampled, correlated data, *Atmos. Chem. Phys.*, 10, 6737–6747, doi:10.5194/acp-10-6737-2010, 2010. 17762

von Hobe, M., Bekki, S., Borrmann, S., Cairo, F., D'Amato, F., Di Donfrancesco, G., Dörnbrack, A., Ebersoldt, A., Ebert, M., Emde, C., Engel, I., Ern, M., Frey, W., Genco, S., Griessbach, S., Grooß, J.-U., Gulde, T., Günther, G., Hösen, E., Hoffmann, L., Homonnai, V., Hoyle, C. R., Isaksen, I. S. A., Jackson, D. R., Jánosi, I. M., Jones, R. L., Kandler, K., Kalicinsky, C., Keil, A., Khaykin, S. M., Khosrawi, F., Kivi, R., Kuttippurath, J., Laube, J. C., Lefèvre, F., Lehmann, R., Ludmann, S., Luo, B. P., Marchand, M., Meyer, J., Mitev, V., Molleker, S., Müller, R., Oelhaf, H., Olschewski, F., Orsolini, Y., Peter, T., Pfeilsticker, K., Piesch, C., Pitts, M. C., Poole, L. R., Pope, F. D., Ravegnani, F., Rex, M., Riese, M., Röckmann, T., Rognerud, B., Roiger, A., Rolf, C., Santee, M. L., Scheibe, M., Schiller, C., Schlager, H., Siciliani de Cumis, M., Sitnikov, N., Søvde, O. A., Spang, R., Spelten, N., Stordal, F., Sumińska-Ebersoldt, O., Ulanovski, A., Ungermann, J., Viciani, S., Volk, C. M., vom Scheidt, M., von der Gathen, P., Walker, K., Wegner, T., Weigel, R., Weinbruch, S., Wetzel, G., Wienhold, F. G., Wohltmann, I., Woiwode, W., Young, I. A. K., Yushkov, V., Zobrist, B., and Stroh, F.: Reconciliation of essential process parameters for an enhanced predictability of Arctic stratospheric ozone loss and its climate interactions (RECONCILE): activities and results, *Atmos. Chem. Phys.*, 13, 9233–9268, doi:10.5194/acp-13-9233-2013, 2013. 17746

Waters, J., Froidevaux, L., Harwood, R. S., Jarnot, R. F., Pickett, H. M., Read, W. G., Siegel, P. H., Cofield, R. E., Filipiak, M. J., Flower, D. A., Holden, J. R., Lau, G. K., Livesey, N. J., Manney, G. L., Pumphrey, H. C., Santee, M. L., Wu, D. L., Cuddy, D. T., Lay, R. R., Loo, M. S., Perun, V. S., Schwartz, M. J., Stek, P. C., Thurstans, R. P., Boyles, M. A., Chandra, K. M., Chavez, M. C., Chen, G. S., Chudasama, B. V., Dodge, R., Fuller, R. A., Girard, M. A., Jiang, J. H., Jiang, Y. B., Knosp, B. W., LaBelle, R. C., Lam, J. C., Lee, K. A., Miller, D., Oswald, J. E., Patel, N. C., Pukala, D. M., Quintero, O., Scaff, D. M., Van Snyder, W., Tope, M. C., Wagner, P. A., and Walch, M. J.: The Earth Observing System Microwave Limb Sounder (EOS MLS) on the Aura satellite, *IEEE T. Geosci. Remote*, 44, 1075–1092, 2006. 17750

Weigel, K., Rozanov, A., Azam, F., Bramstedt, K., Damadeo, R., Eichmann, K.-U., Gebhardt, C., Hurst, D., Krämer, M., Lossow, S., Read, W., Spelten, N., Stiller, G. P., Walker, K. A., We-

ber, M., Bovensmann, H., and Burrows, J. P.: UTLS Water vapour from SCIAMACHY limb measurements V3.01 (2002–2012), Atmos. Meas. Tech. Discuss., in press, 2015. 17752  
Winker, D. M., Hunt, W. H., and McGill, M.: Initial performance assessment of CALIOP, Geophys. Res. Lett., 34, L19803, doi:10.1029/2007GL030135, 2007. 17753

ACPD

15, 17743–17796, 2015

## Sensitivity of PSCs to H<sub>2</sub>O and temperature changes

F. Khosrawi et al.

Title Page

Abstract

Introduction

Conclusions

References

Tables

Figures



Back

Close

Full Screen / Esc

Printer-friendly Version

Interactive Discussion







## Sensitivity of PSCs to H<sub>2</sub>O and temperature changes

F. Khosrawi et al.

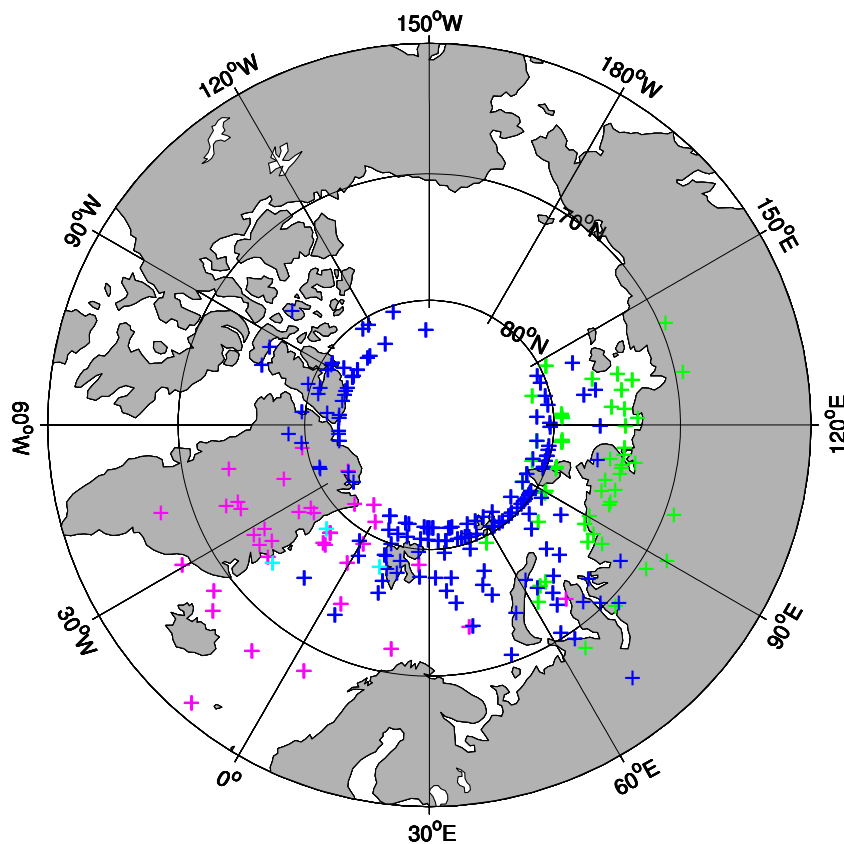


**Figure 1.** Start points where the back trajectories were started according to the PSCs observed by CALIPSO during the four cold phases during the Arctic winter 2010/11 (Phase 1: 23 December–8 January (magenta), Phase 2: 20–28 January (green), Phase 3: 5–27 February (blue) and Phase 4: 5–18 March (cyan)).

[Title Page](#)[Abstract](#)[Introduction](#)[Conclusions](#)[References](#)[Tables](#)[Figures](#)[Back](#)[Close](#)[Full Screen / Esc](#)[Printer-friendly Version](#)[Interactive Discussion](#)



Sensitivity of PSCs to H<sub>2</sub>O and temperature changes

F. Khosrawi et al.

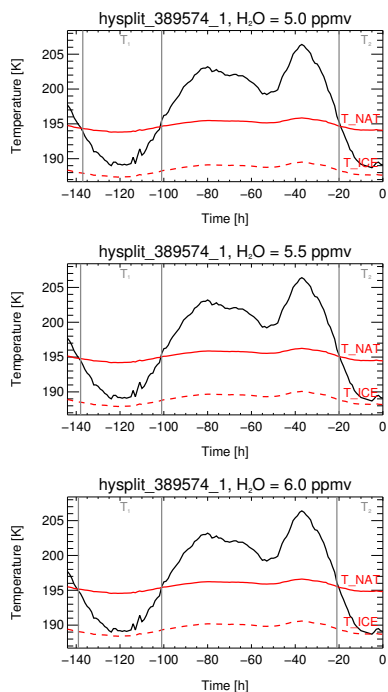


**Figure 3.** Temperature history of the back trajectory calculated with HYSPLIT based on the PSC measured by CALIPSO on 26 February 2011 (back trajectory started at 20 km at 00:00 UTC). Top: for a typical H<sub>2</sub>O mixing ratio of 5 ppmv in the polar lower stratosphere, middle: for an H<sub>2</sub>O enhancement of 0.5 ppmv (5.5 ppmv), bottom: for an H<sub>2</sub>O enhancement of 1 ppmv (6 ppmv). The NAT existence temperature  $T_{\text{NAT}}$  and ice formation temperature  $T_{\text{ice}}$  are given as solid and dashed lines, respectively. Temperatures drop below the NAT formation temperature at time periods  $t = -140$  to  $-100$  h and  $t = -20$  to 0 h. The temperature ranges during these time periods are denoted by  $T_1$  and  $T_2$ , respectively (grey solid lines).

Title Page	
Abstract	Introduction
Conclusions	References
Tables	Figures
◀	▶
◀	▶
Back	Close
Full Screen / Esc	
Printer-friendly Version	
Interactive Discussion	





Sensitivity of PSCs to  $\text{H}_2\text{O}$  and temperature changes

F. Khosrawi et al.

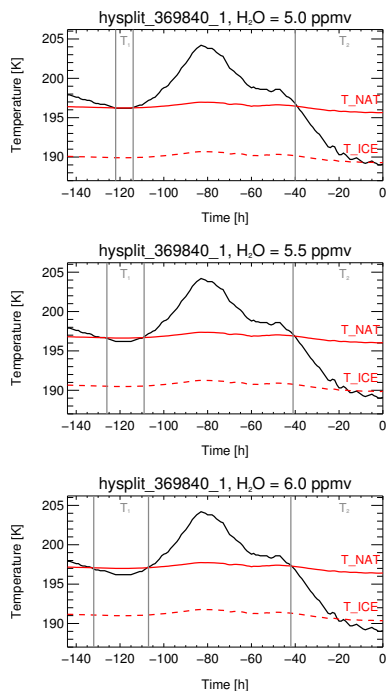


**Figure 5.** Temperature history of the back trajectory calculated with HYSPLIT based on the PSC measured with CALIPSO on 23 January 2011 (back trajectory started at 18 km at 20:00 UTC). Top: for a typical  $\text{H}_2\text{O}$  mixing ratio of 5 ppmv in the polar lower stratosphere, middle: for an  $\text{H}_2\text{O}$  enhancement of 0.5 ppmv (5.5 ppmv), bottom: for an  $\text{H}_2\text{O}$  enhancement of 1 ppmv (6 ppmv). The NAT existence temperature  $T_{\text{NAT}}$  and ice formation temperature  $T_{\text{ice}}$  are given as solid and dashed lines, respectively. Temperatures drop below the NAT formation temperature at time periods  $t = -135$  to  $-105$  h and  $t = -45$  to 0 h. The temperature ranges during these time periods are denoted by  $T_1$  and  $T_2$ , respectively (grey solid lines).

Sensitivity of PSCs to H<sub>2</sub>O and temperature changes

F. Khosrawi et al.

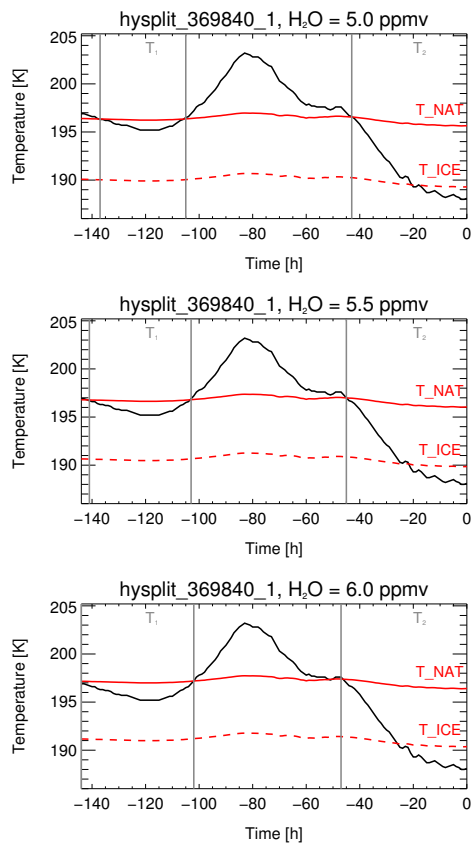


**Figure 6.** Same as Fig. 5 but with an additional temperature decrease along the back trajectory of 1 K.

[Title Page](#)[Abstract](#)[Introduction](#)[Conclusions](#)[References](#)[Tables](#)[Figures](#)[◀](#)[▶](#)[◀](#)[▶](#)[Back](#)[Close](#)[Full Screen / Esc](#)[Printer-friendly Version](#)[Interactive Discussion](#)

Sensitivity of PSCs to H<sub>2</sub>O and temperature changes

F. Khosrawi et al.

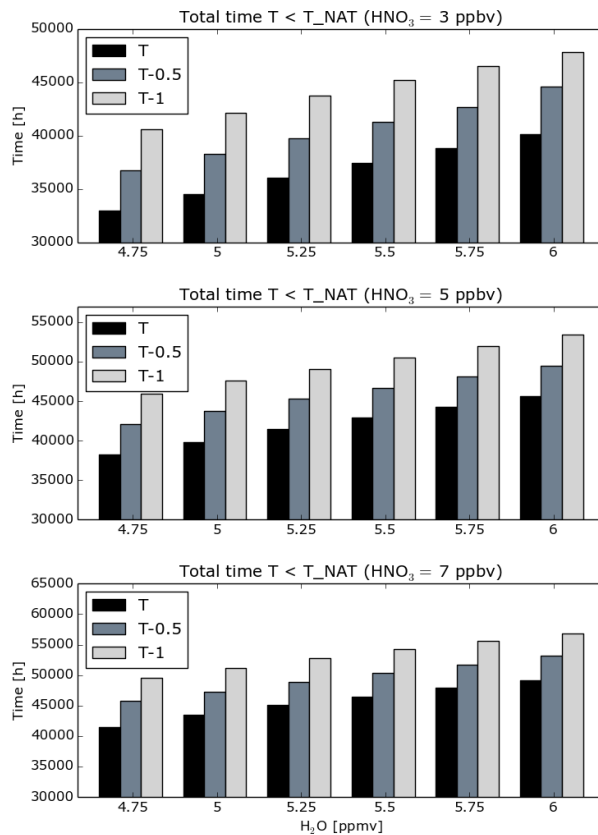


**Figure 7.** Histograms of the total time where the temperature along the back trajectory is below the NAT existence threshold temperature (sum over all 738 back trajectories) for a stratospheric H<sub>2</sub>O mixing ratios of 4.75, 5.0, 5.25, 5.5 and 6.0 ppmv. The calculation was performed assuming an HNO<sub>3</sub> mixing ratio of 3 (top), 5 (middle) and 7 ppbv (bottom). Note the different scales of the subfigures (y axes).

Sensitivity of PSCs to H<sub>2</sub>O and temperature changes

F. Khosrawi et al.

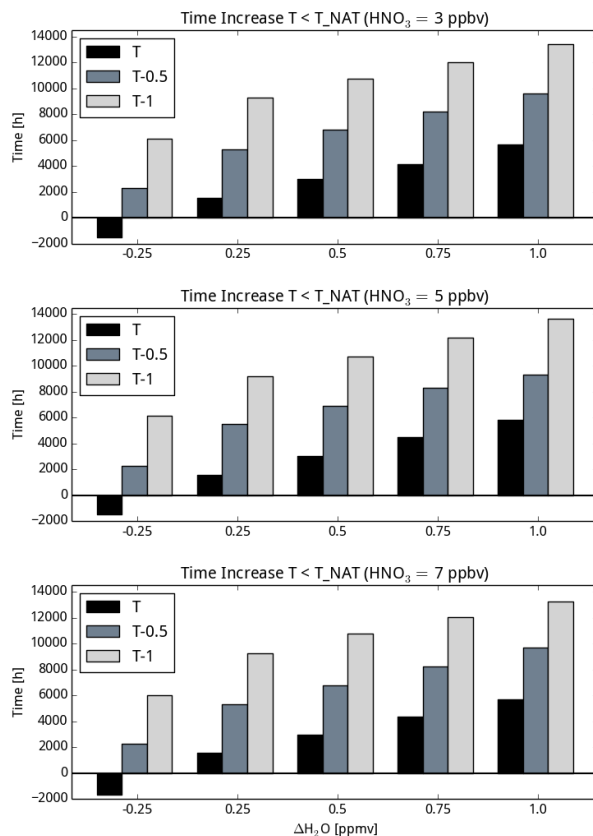


**Figure 8.** Histogram of increase in time where the temperature along the back trajectory is below the threshold temperature (sum over all 738 back trajectories) for a stratospheric H<sub>2</sub>O increase of 0.25, 0.5, 0.75 and 1.0 ppmv, respectively, and for a stratospheric H<sub>2</sub>O decrease of 0.25 ppmv. The calculation was performed assuming an HNO<sub>3</sub> mixing ratio of 3 (top), 5 (middle) and 7 ppbv (bottom).

## Sensitivity of PSCs to H<sub>2</sub>O and temperature changes

F. Khosrawi et al.

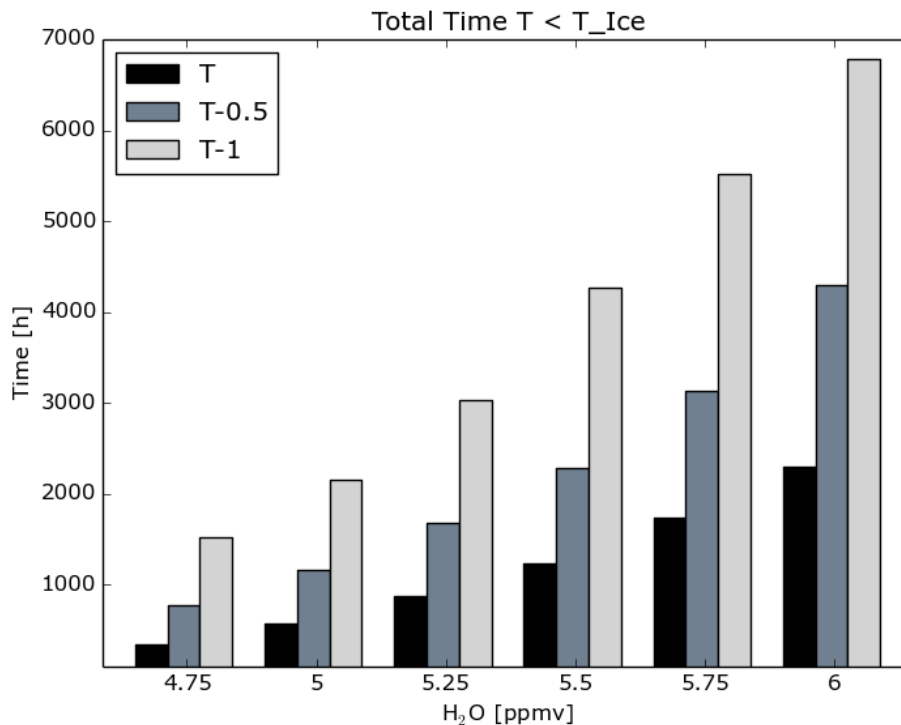


**Figure 9.** Histogram of total time where the temperature along the back trajectory is below the ice formation threshold temperature (sum over all 738 back trajectories) for a stratospheric H<sub>2</sub>O increase of 4.75, 5.0, 5.25, 5.5, 5.75 and 6.0 ppmv.

## Sensitivity of PSCs to H<sub>2</sub>O and temperature changes

F. Khosrawi et al.

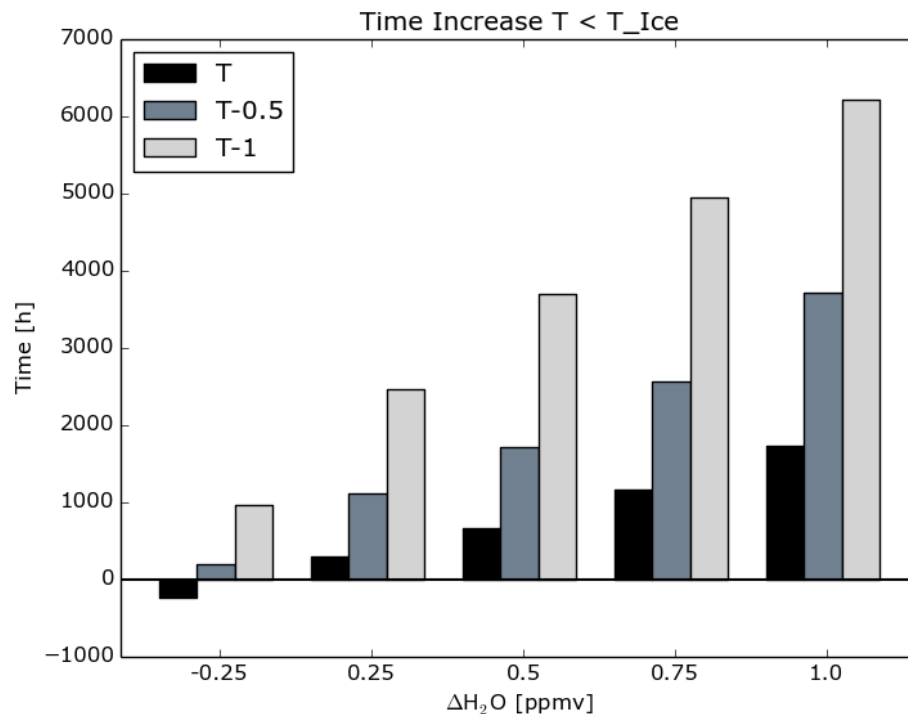


**Figure 10.** Histogram of increase in time where the temperature along the back trajectory is below the ice formation threshold temperature (sum over all 738 back trajectories) for a stratospheric H<sub>2</sub>O increase of 0.25, 0.5, 0.75 and 1.0 ppmv, respectively, and for a stratospheric H<sub>2</sub>O decrease of 0.25 ppmv.

Title Page

Abstract

Introduction

Conclusions

References

Tables

Figures



Back

Close

Full Screen / Esc

Printer-friendly Version

Interactive Discussion



## Sensitivity of PSCs to H<sub>2</sub>O and temperature changes

F. Khosrawi et al.

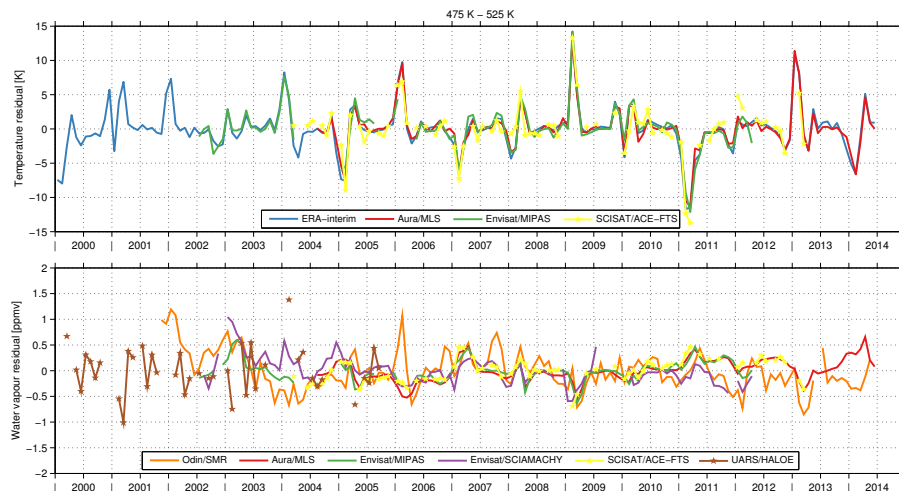


**Figure 11.** Anomaly of the monthly mean temperature (top) and water vapour for the polar regions at equivalent latitudes (70 to 90° N). The data were averaged within the potential temperature layers 475–525 K (18–22 km). Shown is is temperature from ERA-interim (blue), Aura/MLS (red), Envisat/MIPAS (green) and SCISAT/ACE-FTS (orange) and water vapour derived from Odin/SMR at 544 GHz band (orange), Aura/MLS (red), Envisat/MIPAS (green), Envisat/SCIAMACHY (purple), SCISAT/ACE-FTS (yellow) and UARS/HALOE (brown).

Title Page

Abstract

Introduction

Conclusions

References

Tables

Figures



Back

Close

Full Screen / Esc

Printer-friendly Version

Interactive Discussion



## Sensitivity of PSCs to H<sub>2</sub>O and temperature changes

F. Khosrawi et al.

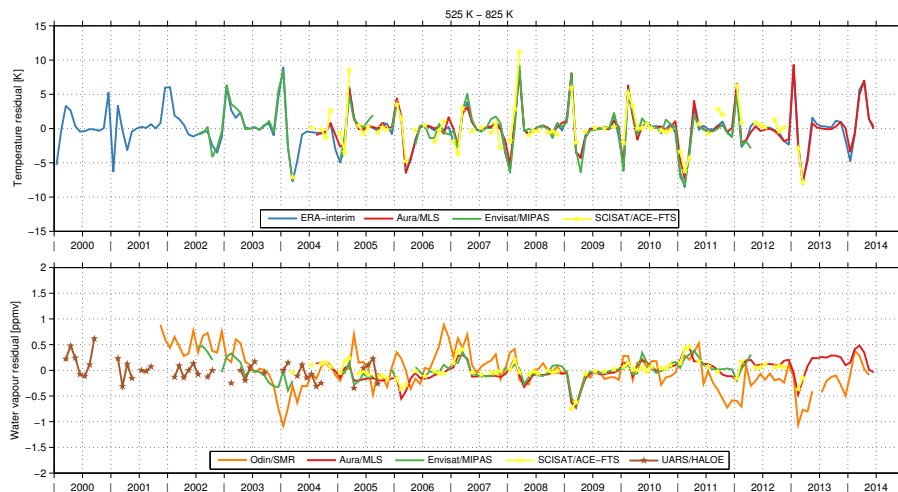
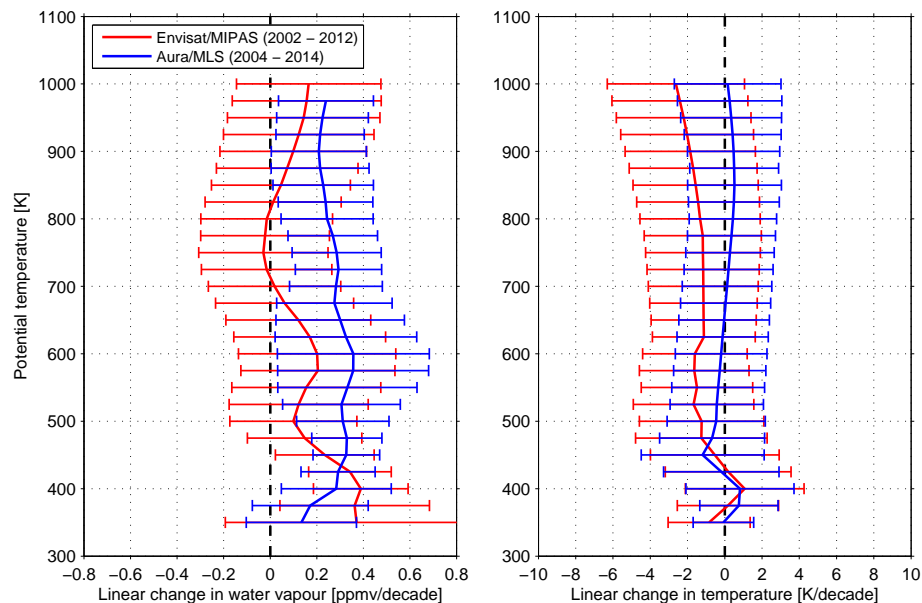


Figure 12. Same as Fig. 2, but for 525–825 K.

[Title Page](#)[Abstract](#)[Introduction](#)[Conclusions](#)[References](#)[Tables](#)[Figures](#)[Back](#)[Close](#)[Full Screen / Esc](#)[Printer-friendly Version](#)[Interactive Discussion](#)

## Sensitivity of PSCs to H<sub>2</sub>O and temperature changes

F. Khosrawi et al.



**Figure 13.** Linear change in water vapour (left) and temperature (right) vs. potential temperature derived from Envisat/MIPAS (2002–2012) and Aura/MLS (2004–2014). For the linear change in water vapour derived from Envisat/MIPAS an offset of 0.1 ppmv between the two measurement periods has been considered. As error bars the  $2\sigma$  uncertainty is given.

[Title Page](#)[Abstract](#)[Introduction](#)[Conclusions](#)[References](#)[Tables](#)[Figures](#)[◀](#)[▶](#)[◀](#)[▶](#)[Back](#)[Close](#)[Full Screen / Esc](#)[Printer-friendly Version](#)[Interactive Discussion](#)

Sensitivity of PSCs to H<sub>2</sub>O and temperature changes

F. Khosrawi et al.

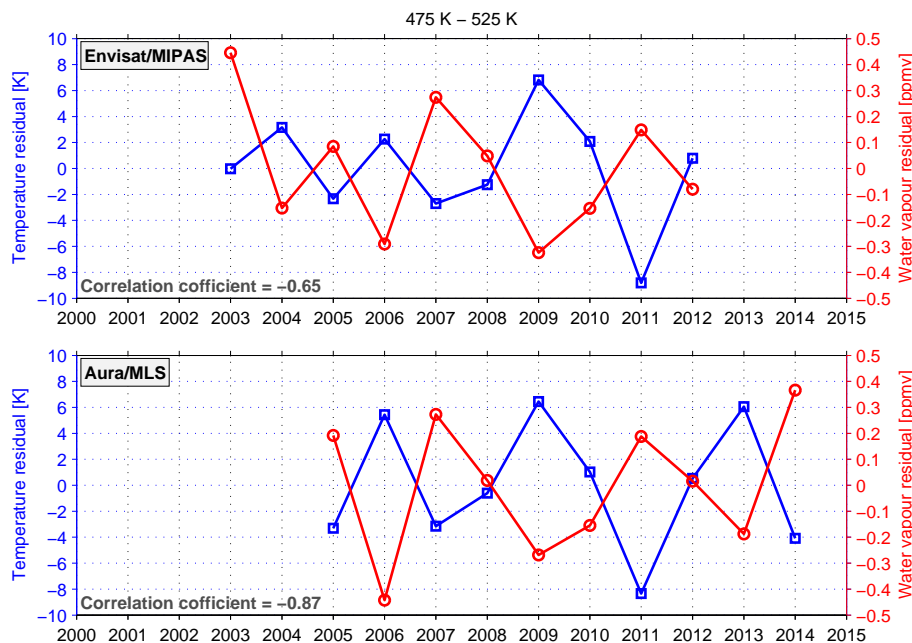


**Figure 14.** Correlation of temperature (blue) and water vapour (red) anomaly derived from Envisat/MIPAS (top) and Aura/MLS (bottom) for potential temperature range 475–525 K (3 month average consisting of the months January, February and March; MIPAS: 2002–2012, MLS: 2005–2014).

[Title Page](#)[Abstract](#)[Introduction](#)[Conclusions](#)[References](#)[Tables](#)[Figures](#)[Back](#)[Close](#)[Full Screen / Esc](#)[Printer-friendly Version](#)[Interactive Discussion](#)

